

# Persistence of a reef fish metapopulation via network connectivity: theory and data

Allison G. Dedrick<sup>a,\*1</sup>

Katrina A. Catalano<sup>a</sup>

Michelle R. Stuart<sup>a</sup>

J. Wilson White<sup>b</sup>

Humberto Montes, Jr.<sup>c</sup>

Malin Pinsky<sup>a</sup>

a. Department of Ecology Evolution and Natural Resources, Rutgers University, 14 College Farm Road, New Brunswick, NJ 08901 USA;

b. Department of Fisheries and Wildlife, Coastal Oregon Marine Experiment Station, Oregon State University, Newport, OR 97365 USA;

c. Visayas State University, Pangasugan, Baybay City, 6521 Leyte, Philippines

\* Corresponding author; e-mail: agdedrick@gmail.com

1. Current address: Stanford Woods Institute for the Environment, Stanford University, Stanford, CA 94305 USA.

**Running title:** (45 characters including spaces) Empirical metapopulation persistence

**Keywords:** metapopulation dynamics, self-persistence, network persistence, *Amphiprion clarkii*, connectivity (5/10)

Current word count: Introduction - 594, Methods - Results

## Abstract

Determining metapopulation persistence requires an understanding of both demographic parameters and connectivity among patches, which is well understood by theory but has proved challenging to test empirically. Here we assessed persistence for a network of patches along a coastline in a metapopulation of yellowtail anemonefish (*Amphiprion clarkii*) using seven years of annual sampling data. We found that this metapopulation produces enough surviving offspring to replace itself but is unlikely to persist in isolation, despite stable abundances through time and replacement of recruits when we include immigration. To persist in isolation, the metapopulation would need to have higher production or different dispersal so as to retain essentially all of the recruits it currently produces. Increased habitat density alone does not ensure persistence. These results show that stable abundance alone is not an indicator of network persistence and emphasize the necessity of untangling demographic and connectivity processes to understand metapopulation dynamics. (149/150 words)

# Introduction

Metapopulation dynamics and persistence depend both on connectivity among patches and on demographic rates in each patch (Hastings and Botsford, 2006; Hanski, 1998). Assessing levels of connectivity and demographic parameters has been particularly challenging for marine species, where much of the movement happens in larval stages when individuals are hard to track and able to travel long distances with ocean currents (White et al., 2019). Driven by both fundamental questions and applied needs (Botsford et al., 2001b; White et al., 2010), a large body of theory has developed to describe how marine metapopulations might persist (Botsford et al., 2019). Testing this theory, however, has been substantially more difficult.

For any population to persist, individuals must on average replace themselves during their lifetime. Assessing replacement must include the demographic processes across the life cycle, including how likely individuals are to survive to the next age or stage, their expected fecundity at each stage, and the survival to recruitment of any offspring produced. In a spatially structured population, we must also consider how the offspring are distributed across space (Hastings and Botsford, 2006).

A metapopulation can persist in two ways: 1) at least one patch achieves replacement in isolation, or 2) patches receive enough recruitment to achieve replacement through multi-generational loops of connectivity with other patches in the metapopulation (Hastings and Botsford, 2006; Burgess et al., 2014). In the first case (termed self-persistence), enough of the reproductive output produced at one patch is retained at the patch for it to persist. In the second (network persistence), closed loops of

connectivity among at least some of the patches - where individuals from one patch settle at another and eventually send offspring back to the first in a future generation - provide the patches with enough recruitment to persist within the network. Theory predicts that habitat patches that are large relative to the mean dispersal distance are likely to be self-persistent (White et al., 2010).

New ways of identifying individuals and determining their origins now allow better measurements of connectivity (Almany et al., 2017; D'Aloia et al., 2013). Additionally, a better appreciation of the relevant population dynamic theory has led to measurement of the appropriate demographic factors necessary to assess persistence in real metapopulations (Carson et al., 2011; Hameed et al., 2016). To date, research has suggested that populations on isolated islands can be self-persistent, which might be expected given that they lack nearby populations with which to exchange larvae and would go locally extinct if they did not achieve replacement Salles et al. (2015). In contrast, small habitat patches spread across a larger reef metapopulation appear to rely on outside input for persistence (Johnson et al., 2018). Persistence, however, has yet to be assessed in the field for an entire continuous marine metapopulation, such as all of the patches along a coastline.

Here, we further our understanding of metapopulation dynamics in a network of patches along a coastline through a study of yellowtail anemonefish (*Amphiprion clarkii*) in the Philippines. We assess persistence for all patches of habitat within a 30 km stretch of coastline, a distance greater than estimates of the mean dispersal distance for this species (Pinsky et al., 2010), suggesting the network may operate as a contained metapopulation. With seven years of annual sampling data, we estimate

long-term persistence metrics and replacement and investigate abundance through time to compare with persistence metrics. We find that even large collections of populations with stable abundances through time are unlikely to persist as an isolated metapopulation and require immigration from outside patches to persist.

## Methods

### Persistence theory and metrics

We considered four primary metrics to assess whether and how the metapopulation was persistent: 1) lifetime recruit production (LRP) to assess whether the metapopulation had enough offspring that survived anywhere to achieve replacement, 3) self-persistence (SP) to assess whether any individual patch could persist in isolation without input from other patches, 3) network persistence ( $\lambda_c$ ) to assess whether the metapopulation was persistent as a connected unit, and 4) local replacement (LR) to assess whether a sufficient number of recruits were retained anywhere within the metapopulation to achieve replacement, without explicitly estimating dispersal. We explain each metric below in detail. To represent the uncertainty in our estimates, we calculated each metric 1000 times, sampling each input parameter from a distribution that represents the uncertainty in each empirical estimate of demographic rates or connectivity (details in A.11). In our results, we show our best estimate of each persistence metric along with the range of uncertainty values.

## Lifetime recruit production

We found the number of recruits an individual recruit will produce (lifetime recruit production,  $LRP_i$ ) by multiplying the patch-specific total number of eggs a recruit-sized individual produces in its lifetime (lifetime egg production, LEP) by the fraction that survive to become recruits (egg-recruit survival,  $S_e$ ) (Fig. D.1):

$$LRP = LEP * S_e. \quad (1)$$

If  $LRP \geq 1$ , individuals produced enough surviving offspring, before considering dispersal, to potentially achieve replacement. If  $LRP < 1$ , the population cannot persist without input from outside patches. We considered all recruits produced by adults in our metapopulation to estimate  $LRP$ , regardless of where they settled. This estimates the potential for the entire metapopulation to persist.

## Self-persistence

A single patch is self-persistent if individuals produced enough offspring that survived to recruitment ( $LRP_i$ ) and settled in the natal patch (probability of dispersal  $p_{i,i}$ ) to replace themselves:

$$SP_i = LRP_i \times p_{i,i}. \quad (2)$$

A patch  $i$  is self-persistent if  $SP_i \geq 1$ . If at least one patch is self-persistent,

the metapopulation as a whole is persistent as well (Hastings and Botsford, 2006; Burgess et al., 2014).

### **Network persistence**

Network persistence explicitly considers dispersal of individuals among patches in addition to the reproduction and survival at each patch. We created the elements of a realized connectivity matrix  $C$  by multiplying dispersal probabilities among pairs of patches by lifetime recruit production (Burgess et al., 2014):

$$C_{i,j} = \text{LRP}_i \times p_{i,j}. \quad (3)$$

The diagonal entries of  $C$  are the self-persistence values for each individual patch ( $\text{SP}_i$ ). Network persistence is the largest real eigenvalue of the realized connectivity matrix  $\lambda_C$ , which must be at least 1 for the network to persist without outside input (Hastings and Botsford, 2006; White et al., 2010; Burgess et al., 2014).

### **Local replacement**

Local replacement (LR) estimates the number of recruits produced per individual that returned to settle within the focal metapopulation (as opposed to LRP, which considers recruits that settle anywhere). We multiplied LEP averaged across sites by the proportion of eggs that survived and returned to recruit at our patches ( $R_e$ ).

$R_e$  is a modification of egg-recruit survival ( $S_e$ ) that implicitly includes dispersal.

$$\text{LR} = \text{LEP} \times R_e. \quad (4)$$

If  $\text{LR} \geq 1$ , enough offspring were locally retained to achieve replacement if they were evenly spread among patches, but the actual dispersal patterns among the metapopulation patches may still prevent replacement.  $\text{LR}$  and  $\lambda_c$  both assess the ability of our patches to persist as an isolated group but  $\text{LR}$  treats the network as one large homogenous patch while  $\lambda_c$  explicitly accounts for the struture and connectivity across patches.

## Study species

We focused on a tropical metapopulation of yellowtail anemonefish (*Amphiprion clarkii*, Fig. 1c). Like many anemonefish species, yellowtail anemonefish have a mutualistic relationship with anemones that house small colonies of fish (Buston, 2003b; Fautin et al., 1992). Yellowtail anemonefish are protandrous hermaphrodites and maintain a size-structured hierarchy; within an anemone, the largest fish is the breeding female, the next largest is the breeding male, and any smaller fish are non-breeding juveniles. The fish move up in rank to become breeders only after the larger fish have died. In the tropical patch reef habitat of the Philippines, yellowtail anemonefish primarily spawn from November to May, laying clutches of benthic eggs that the parents protect and tend (Ochi, 1989; Holtswarth et al., 2017). Larvae hatch after about six days and spend 7-10 days in the water column before returning to

reef habitat to settle in an anemone (Fautin et al., 1992).

Anemonefish are well-suited to metapopulation studies because dispersal only occurs during the larval phase and adults have limited movement on discrete habitat patches (anemones) (e.g. Buston and DAloia, 2013; Salles et al., 2015; Almany et al., 2017). Yellowtail anemonefish tend to behave more like larger reef fishes, with wider-ranging territories and stronger swimming abilities (Hattori and Yanagisawa, 1991; Ochi, 1989), than the smaller *A. percula* commonly used in metapopulation studies (e.g. Buston et al., 2011; Salles et al., 2015). As we show later, survival in yellowtail anemonefish is also lower than *A. percula* and more similar to other damselfishes.

## Field data collection

We focused on a set of nineteen reef patches spanning 30 km along the western coast of Leyte island facing the Camotes Sea in the Philippines (Fig. 1a). The habitat patches cover approximately 20% of the sampling region and consist of rocky patches of coral reef separated by sand flats (Fig. 1a,b). To the north, the patches are isolated from nearby habitat with no substantial reef habitat for at least 20 km. Located near a populated coastline, the region experiences anthropogenic effects including fishing, pollution, and runoff from agriculture and a nearby riverbed gravel mine.

From 2012-2018, we annually sampled fish and habitat at most patches (Table A3). Divers using SCUBA and tethered to GPS readers swam the extent of each patch and visited anemones inhabited by yellowtail anemonefish. We noted but did not include in analysis anemones inhabited by other anemonefish species. At each anemone, the divers caught fish 3.5 cm and larger, took a small tissue sample,

measured fork length, and noted tail color as an indicator of life stage. Starting in 2015, fish 6.0 cm and larger were also tagged with a passive integrated transponder (PIT) tag unless already tagged. Divers also looked for eggs around each anemone and measured and photographed any clutches found. In total, we took fin clips from and genotyped 2407 fish and PIT-tagged 1930 fish across all years and patches combined, marking 3053 individual fish.

## Estimating demographic and dispersal parameters from empirical data

### Parentage analysis and dispersal kernel

Over seven years of sampling, we genotyped 1719 potential parents and 785 juveniles and found 62 parent-offspring matches (Catalano et al., in prep). We used a distance-based dispersal kernel fit from the parent-offspring matches (Catalano et al., in prep; Bode et al., 2018), where the relative dispersal  $p(d)$  is a function of distance  $d$  in kilometers and parameters  $\theta = 1.19$  and  $z = e^{k_d=-2.33}$  that control the shape and scale of the kernel (Table A1):  $p(d) = ze^{-(zd)^\theta}$ . The dispersal kernel estimates the relative dispersal by distance for fish that have survived and recruited so does not separately estimate pre-settlement mortality. To find the probability of fish dispersing among our patches, we numerically integrated the dispersal kernel using the distance from the middle of the origin patch ( $i$ ) to the closest ( $d_1$ ) and farthest ( $d_2$ ) bounds of the destination patch ( $j$ ):

$$p_{i,j}(d) = \int_{d_1}^{d_2} z e^{-(zd)^\theta} dd. \quad (5)$$

## Growth and survival: mark-recapture analyses

Fish marked through genetic samples and PIT tags allowed us to estimate growth and survival through mark-recapture. In total, we had 3053 marked fish with size and stage data for each capture time.

For growth, we estimated the parameters of a von Bertalanffy growth curve in the growth increment form relating the length at first capture  $L_t$  to the length at a later capture  $L_{t+1}$  (Hart and Chute, 2009), where  $L_\infty$  is the average asymptotic maximum size across the metapopulation and  $K$  is the growth rate:

$$\begin{aligned} L_{t+1} &= L_t + (L_\infty - L_t)[1 - e^{(-K)}] \\ &= e^{(-K)}L_t + L_\infty[1 - e^{(-K)}]. \end{aligned} \quad (6)$$

From the slope  $m = e^{(-K)}$  and y-intercept  $b = L_\infty[1 - e^{(-K)}]$ , we calculated the von Bertalanffy parameters, such that  $K = -\ln m$  and  $L_\infty = \frac{b}{(1-m)}$  (Hart and Chute, 2009). We used the first and second capture lengths for fish that were recaptured after a year (within 345 to 385 days) to estimate  $L_\infty$  and  $K$ . For fish recaptured more than once, we randomly selected only one recapture period from each to use to estimate the von Bertalanffy parameters and repeated the random selection and estimate 1000 times. We found the mean estimates ( $L_\infty = 10.70$  cm,  $K = 0.864$ ) and mean

standard error of those fits, then sampled from within that range to generate a set of von Bertalanffy growth curves to use in our LEP calculations (Fig. 2b, Table A1, A.3).

We used the full set of marked fish to estimate annual survival  $\phi$  and probability of recapture  $p_r$  using the mark-recapture program MARK implemented in R through the package `RMark` (Laake, 2013). We fit several models with year, size, and patch effects on the probability of survival on a log-odds scale (see full list in Table A2), and the best fit had an effect of patch and a positive effect of size (Table A1, Figs. 2c, D.5, A.3).

## Fecundity

Fecundity is size-dependent, based on field data, with larger females producing more eggs (eqn. A.1, A.2).

## Lifetime egg production

We used an integral projection model (IPM) (Ellner et al., 2016) with size as the continuous structuring trait  $z$  to estimate lifetime egg production (LEP). We initialized the IPM with one recruit-sized individual (recruit defined in A.1) at the initial annual time step ( $t = 0$ ), then projected forward for 100 years. We used the size-dependent survival (eqn. B.1) and growth (eqn. 6) functions as the probability density functions in the kernel to describe the survival and growth of the individual into the next time step. The size distribution ( $v_z$ ) at each time step represents the probability that the individual has survived and grown into each of the possible size

categories, ranging from a minimum of  $L_s = 0$  cm to a maximum of  $U_s = 15$  cm divided into 100 equal size bins.

We then multiplied the size-distribution  $v_z$  at each time by the size-dependent fecundity  $f_z$  (eqn. A.1) to get the total number of eggs produced at each time step. Integrating across time and size gave the total number of eggs one individual produced in its lifetime (details in A.4):

$$\text{LEP} = \int_{t=0}^{100} \int_{z=L_s}^{z=U_s} v_{z,t} f_z dz dt. \quad (7)$$

We only considered reproductive effort once the fish was female and used the average size of first female observation for recaptured fish as the transition size  $L_f = 9.32$  cm.

### Survival from egg to recruit

We estimated survival from egg to recruit ( $S_e$ ) (recruit defined in A.1) using parentage matches to find the number of surviving recruits produced by genotyped parents (similar to Johnson et al., 2018). We scaled the number of offspring we assigned back to parents ( $R_m = 62$ ) to account for offspring missed by our sampling ( $P_h$ ,  $P_c$ ,  $P_d$ , and  $P_s$ , described below and in Fig. D.2), then divided by the number of eggs produced by genotyped parents:

$$S_e = \frac{\frac{R_m}{P_h P_c P_d P_s}}{N_g \text{LEP}_p}, \quad (8)$$

where  $N_g$  (=1719) was the number of genotyped parents,  $\text{LEP}_p$  was the expected

LEP for a fish of parent size  $p$  ( $=6.0\text{cm}$ ) rather than for a recruit,  $P_h$  ( $=0.41$ ) was the proportion of habitat in our patches that we sampled over time (details in A.6),  $P_c$  ( $=0.56$ ) was the probability of capturing a fish if we sampled its anemone (see A.7 for details),  $P_d$  ( $=0.57$ ) was the proportion of the total dispersal kernel area from each of our patches covered by our sampling region (see A.8), and  $P_s$  ( $=0.20$ ) was the proportion of suitable habitat in our sampling region (see A.9).

To estimate the survival and retention of recruits back to our patches (needed for local replacement, LR eqn. 4), we scaled only by  $P_h$  and  $P_c$ :  $R_e = \frac{\frac{R_m}{P_h P_c}}{N_g \text{LEP}_p}$ .

### **Accounting for density-dependence**

Ideally we would assess persistence metrics when the population is at low abundance and not limited by density dependence because persistence is defined as having positive population growth at low density; at high density the growth rate will slow to zero. Density dependence is particularly clear in anemonefish, which have strong social hierarchies; juveniles on an anemone will prevent others from settling there as well (seen in *A. percula*, Buston, 2003a). Each anemone, therefore, can house only one recently settled anemonefish. This density-dependent mortality will artificially reduce the apparent survival of new recruits, biasing persistence metrics. We account for this effect by scaling up our estimate of recruits (the numerator of eqn. 8) by the proportional increase (DD) in unoccupied anemones if all of the anemones occupied by yellowtail anemonefish were unoccupied, where  $p_A$  is the proportion of anemones occupied by yellowtail anemonefish and  $p_U$  is the proportion of unoccupied anemones:  $\text{DD} = \frac{(p_U + p_A)}{p_U} = 1.71$ . We present results with this density-dependence

modification in the main text and without in the appendix (with subscript DD, Figs. D.8, D.9).

### Estimated abundance over time

We examined trends in abundance of breeding females at each patch over time ( $F_{i,t}$ ) to compare to our replacement-based persistence estimates. As with offspring, we scaled up the number of females caught ( $F_c$ ) at each patch  $i$  in each sampling year  $t$  by the proportion of habitat sampled in that patch and year ( $P_{h_{i,t}}$ ) and by the probability of capturing a fish  $P_c$ :

$$F_{i,t} = \frac{F_{c_{i,t}}}{P_{h_{i,t}} P_c} \quad (9)$$

We fit a mixed effects model to estimate the number of fish in each year as a Poisson variable  $\lambda_a$  with effect  $m_t$  of year  $t$  and with patch as a random effect  $m_i$  using the package `lme4` in R (Bates et al., 2015):

$$\begin{aligned} F_{i,0} &\sim Poisson(\lambda_a) \\ F_{i,t} &= (\lambda_a + m_i)m_t t. \end{aligned} \quad (10)$$

We estimated  $\lambda_a$  for an average patch as well as the individual patches.

### Sensitivity to percent habitat, region width, and larval navigation

Patch width and the proportion of coastline that is habitat affect metapopulation persistence (with persistence expected when patch width is greater than mean dispersal distance or at least 35% of the coastline is habitat, Botsford et al. (2001a)), so we tested the sensitivity of metapopulation persistence to the proportion habitat and width of the sampling region. We varied the proportion of habitat and the overall width of the metapopulation region using 19 equally sized and spaced patches with average adult survival. We created connectivity matrices using the new distances between patches and otherwise used the original parameter values and uncertainty sets.

We also tested sensitivity to the ability of larvae to navigate to habitat by adding a buffer to the edges of the destination patches when integrating the dispersal kernel and adjusting the scaling parameter  $P_s$  (eqn. 8) to account for fewer larvae being lost between patches (details in A.10.0.1).

## Results

For demographic inputs to the persistence metrics, we found that average asymptotic maximum size ( $L_\infty$ ) was 10.70, and annual survival increased with fish size and varied across patches (Figs. 2c, D.5). We estimated average lifetime recruit production (LRP) across patches to be 1.45 [0.62, 7.78] with uncertainty (Fig. 3c), with best estimates of  $LRP_i$  at individual patches ranging from 0 to 3.5. Average across patches, 94% of LRP estimates were  $\geq 1$ . This means that individuals produced

enough surviving offspring to be able to replace themselves. However, LRP does not tell us whether those offspring settled within our sample patches and contributed to persistence.

Considering retention of larvae at individual patches, we did not find any patches with a best estimate of  $SP_i \geq 1$  (Fig. 4a), suggesting that no patch could persist in isolation. The patch Haina ( $SP_i = 0.047$  [9.5e-05, 0.60]) had the largest SP, but none of the estimates with uncertainty are  $\geq 1$ . The large uncertainty at Caridad Cemetery stems from the lack of recaptures of marked fish and therefore the high uncertainty in adult survival.

Most of the connectivity in the metapopulation occurred among the patches in the northern and southern parts of our sample area, from Palanas to Caridad Cemetery and from Tomakin Dako to Sitio Baybayon (Fig. 4b), where the patches tend to be larger, have higher abundances, and have higher survival (Fig. D.5). The patches with the highest abundances are at the edges of our sampling region, and have higher than average LRP, which means a substantial fraction of the recruits they produce could be exported away from our patches rather than into our sampling region.

For network persistence, our best estimate of  $\lambda_c$  was 0.15 [0.064, 1.54], with only a 0.5% chance  $\lambda_c \geq 1 = 0.005$  (Fig. 4c). Network persistence for this metapopulation is therefore highly unlikely but not impossible. Our estimate of local replacement LR was 0.16 [0.07, 0.88], also suggesting lack of independent persistence of our group of patches and very similar to our  $\lambda_c$  estimate. While both LR and  $\lambda_c$  provide information on the ability of our patches to persist as an isolated group, they differ in their assumption of the structure of the population. LR estimates the number of recruits

individuals at our patches produced that settled within our patches, assuming the network of patches was a single well-mixed unit, while  $\lambda_c$  accounts for the spatial structure and multi-generation dynamics.

Our estimated abundance of females over time had a slight positive trend for the average patch ( $m_t = 1.08$ , Fig. 3a), suggesting a slight increase in population size through time. Most individual patches also showed a slight positive trend in female abundance through time, though one large patch showed declines (Fig. 3a, Fig. D.7s). Therefore, while the metapopulation did not appear to be network persistent, it also did not appear to be going extinct.

This was further confirmed when we calculated LR using all recruits arriving to our patches, rather than just those originating there, assessing whether there was replacement with immigrants included. LR with immigrants gave a best estimate  $> 1$  (2.08 with 99.8% estimates  $\geq 1$ ), also suggesting that there was recruit-recruit replacement for the metapopulation when outside recruits were included.

We then examined what conditions could allow this metapopulation to reach persistence. With our existing patch configuration and dispersal kernel, we would need a LRP  $\geq 8.8$  to reach network persistence. In turn, this would require an egg-recruit survival ( $S_e$ )  $\geq 0.012$  or LEP  $\geq 4406$ . Including all arriving recruits as offspring, not just those originating within the metapopulation, LRP would be 10.43, sufficient for persistence.

Another route to persistence would be with a different dispersal matrix. If essentially all recruits produced from our patches landed on one of the outer patches (i.e., none lost to sandy areas between patches or to habitat beyond our study region),

the metapopulation would be network persistent because  $\text{LRP} \geq 1$ . With observed dispersal, however, retaining all recruits is difficult to achieve. The coastline has a low fraction of habitat (currently about 20%), but increasing this even to 100% did not achieve network persistence with certainty ( $\lambda_c = 0.95$ , with only 59% of the estimates  $\geq 1$ , Fig. 5a). Essentially all of the offspring produced by the metapopulation need to be retained for persistence in the best estimate and even with 100% habitat, many were exported outside of the region. Widening the region at the same habitat density also did not contribute to persistence (Fig. 5b) but persistence became likely for a wider region of 100% habitat (best estimate  $> 1$  at about 33 km, Fig. 5c). Allowing for larval navigation hardly changed our persistence estimates (Fig. 5d), as the larger effective area for each patch was essentially offset by removing that area from the scaling that accounted for larval losses to non-habitat ( $P_s$  in eqn. 8).

## Discussion

In this first assessment of demographic persistence of a coastal marine metapopulation, we did not find strong evidence for either self-persistence of an individual patch or network persistence of the entire 30 km system as an isolated region. This inability to persist as an isolated region does not mean that the metapopulation is declining, however. Population trends - both abundance over time and replacement of recruits with immigrants included - find that population levels are stable or increasing slightly. Taken together, these metrics suggest that the region has a stable population on average but requires input of immigrants to persist. Despite encompassing a distance larger than mean dispersal, the coastline only persists as part of

a larger metapopulation.

For the anemonefish metapopulation to persist as an isolated network, either the number of surviving recruits produced by an average recruit (LRP) would need to be about six times higher (about XX) or more recruits would need to be retained within the region. This higher LRP value is similar to estimates of lifetime reproductive success that include dispersal to the natal reef in a clownfish on an isolated island (Salles et al., 2020), suggesting it is not an unreasonable level of production. Habitat quality affects production in reef fishes (e.g., Salles et al., 2020; Hayashi et al., 2019), and our study system is near a populated coastline and experiences anthropogenic effects, including pollution and silt from a riverbed gravel mine. Adult survival, for example, was lower at the two patches just downstream of the gravel mine (N. and S. Magbangon in Fig. D.5), with impacts on  $LEP_i$  and therefore  $LRP_i$ .

Alternately, higher connectivity and retention of offspring among patches could lead to network persistence. Though lack of sufficient connectivity and retention is thought to inhibit network persistence in other systems (e.g., a collection of reserves for eastern oysters (*Crassostrea virginica*) in the Pamlico Sound in North Carolina; Puckett and Eggleston, 2016), low production of surviving recruits due to poor habitat quality seems the more likely explanation in our system. Our dispersal kernel is comparable to those estimated for other species of reef fish, both similar in shape (e.g., Harrison et al., 2012; DAloia et al., 2015) and with a mean dispersal distance of a similar range to that estimated for *A. percula* in Kimbe Bay (13.3 and 18.9 km compared to our estimate of 8.2 km; Almany et al., 2017), which has been found to be persistent without input from outside reefs (Salles et al., 2015).

We do not find clear evidence for network persistence despite estimates of the mean dispersal distance of *A. clarkii* from previous genetic work (9 km, Pinsky et al., 2010) and from our samples (8.2 km, Catalano et al., in prep) that are well within the 30 km span of our patches. The length of the metapopulation is more than twice the mean dispersal distance, usually sufficient for persistence of a population in an isolated habitat patch (e.g., Lockwood et al., 2002). However, the metapopulation contains only about 20% habitat, rather than a continuous stretch, which may be too low to support network persistence. Habitat quality and extent in our region has likely been declining in recent decades. The region was hit in 2013 by Typhoon Haiyan, one of the strongest typhoons ever to make landfall, which destroyed reef habitat, including one of our northern sampling patches. Fishers also noticed prior habitat changes when asked in the early 2000s (Jennifer Selgrehth, pers. comm.). Finally, agriculture has spread over much of the steep mountain slopes immediately east of the metapopulation, possibly leading to extensive runoff over historical time and loss of reef habitat along this coastline. Our simulations suggest that even 100% habitat in our sampling region does not guarantee network persistence.

In addition, individual patches are too small to reach self-persistence. The largest patch, Haina, is only 0.8km wide, about 10 times smaller than the mean dispersal distance. This is in contrast to findings on isolated reefs surrounding Kimbe Island, however, where several anemonefish subpopulations in lagoons of similar size as our patches were found self-persistent (Salles et al., 2015). The suggestion of a habitat shortage in our sampling region is partially dependent on our assumption that larvae land in non-habitat between patches and die. Larvae have some navigational and

habitat-finding capabilities (e.g. Elliott et al., 1995; Fisher, 2005), so we could be underestimating their ability to find habitat in our calculations, which would decrease the amount of habitat required for network persistence.

We suggest that this metapopulation is a sink area of a larger metapopulation but the area required for the larger persistent metapopulation depends on the production and connectivity of outside patches. If surrounding patch populations have a similar LRP and level of connectivity as our patches, increasing the area of the network to include them also would not achieve network persistence. If nearby patches have higher egg production or egg-recruit survival, however, it might not take much of an increase in area considered to create a persistent network. Nearby reef patches such as Cuatro Islas, for example, with higher coral cover and less silt, could have higher survival of fish and be contributing recruits to our patches.

An alternative to our sampled patches existing as a sink portion of a larger metapopulation is that variability in demography or dispersal on a longer scale than our sampling time could lead to persistence (similar to the storage effect, Warner and Chesson, 1985) For example, rockfish on the west coast of the United States have highly variable and episodic recruitment, where successful recruitment events occur on the decadal scale and sustain the population until the next strong recruitment event (e.g., Tolimieri and Levin, 2005). Though perhaps not as extreme as in the California Current system, ocean connectivity is still variable in the Coral Triangle region surrounding our study patches, with estimates suggesting that 20 year simulations are necessary to capture the full extent (Thompson et al., 2018). Our study, though relatively long term, could have missed a particularly strong recruitment

event that would enable local persistence of the set of populations we sampled.

Though we estimate abundance trends and do not find overall declines, it is possible we could have missed declines due to our sampling design. Our sampling study was designed for mark-recapture analyses rather than a comprehensive habitat or abundance estimate so we did not sample all areas of all patches each year. We scaled up the number of fish we caught to account for those we missed using the proportion of tagged anemones we visited, which assumes that all tagged anemones are equally likely to be sampled. In reality, tags that no longer have anemones next to them are likely harder to find and sample. If anemones are disappearing over time at our patches, we might be overestimating the number of fish present and missing population declines at our patches that would mean lack of persistence even with outside input. Properly accounting for such uncertainties, and characterizing uncertainty in our parameter estimates, is an important part of persistence estimation.

Persistence criteria (Hastings and Botsford, 2006; Burgess et al., 2014) ask whether a population at low abundance can grow and recover rather than going extinct. Density-dependence is often ignored at low abundances (Botsford et al., 2019) so is not explicitly considered in persistence metrics. In real populations, however, it can be challenging to estimate density-independent demographic rates, as density-dependence is occurring in the population as it is sampled in processes such as dispersal (e.g. in butterflies, Nowicki and Vrabec, 2011) and fecundity (e.g. in warblers, Rodenhouse et al., 2003). In yellowtail anemonefish, density dependence is likely most important immediately post-settlement, as it is for many species (e.g. corals, trees, and butterflies: Vermeij and Sandin, 2008; Harms et al., 2000; Nowicki

et al., 2009), but could continue to be important throughout the life history due to social hierarchies in anemonefish colonies (e.g. Buston and Elith, 2011). To avoid competition within the colony, fish in the pre-reproductive queue may have lower growth and survival than fish alone on an anemone (seen in *A. percula*, Buston, 2003a,b), suggesting higher growth and survival, and therefore LRP, in the absence of density-dependence.

Understanding persistence is critical for the management of spatial populations, such as siting marine protected areas (e.g., Kaplan et al., 2009), assessing habitat fragmentation risks (e.g., Smith and Hellmann, 2002; Fahrig, 2001) and conserving species in the face of climate change (e.g., Coleman et al., 2017; Fuller et al., 2015). Though models and theory provide us with expectations, we are only recently beginning to be able to tackle these questions of persistence empirically in model systems such as clownfish and other sedentary tropical reef fish (e.g., Salles et al., 2015; Johnson et al., 2018). With parentage analyses now being extended to temperate marine species (e.g., Baetscher et al., 2019) and a better understanding of how biophysical models compare to larval dispersal patterns (Bode et al., 2019) we are beginning to move beyond model species and investigate persistence in harvested and spatially-managed systems (e.g., Garavelli et al., 2018). Our study shows the importance of long term sampling and careful consideration of the different demographic processes that affect our metric calculations, such as density-dependence and sampling biases, to distinguish persistence ability from population trajectories and understand marine population dynamics in empirical systems.

## Figures

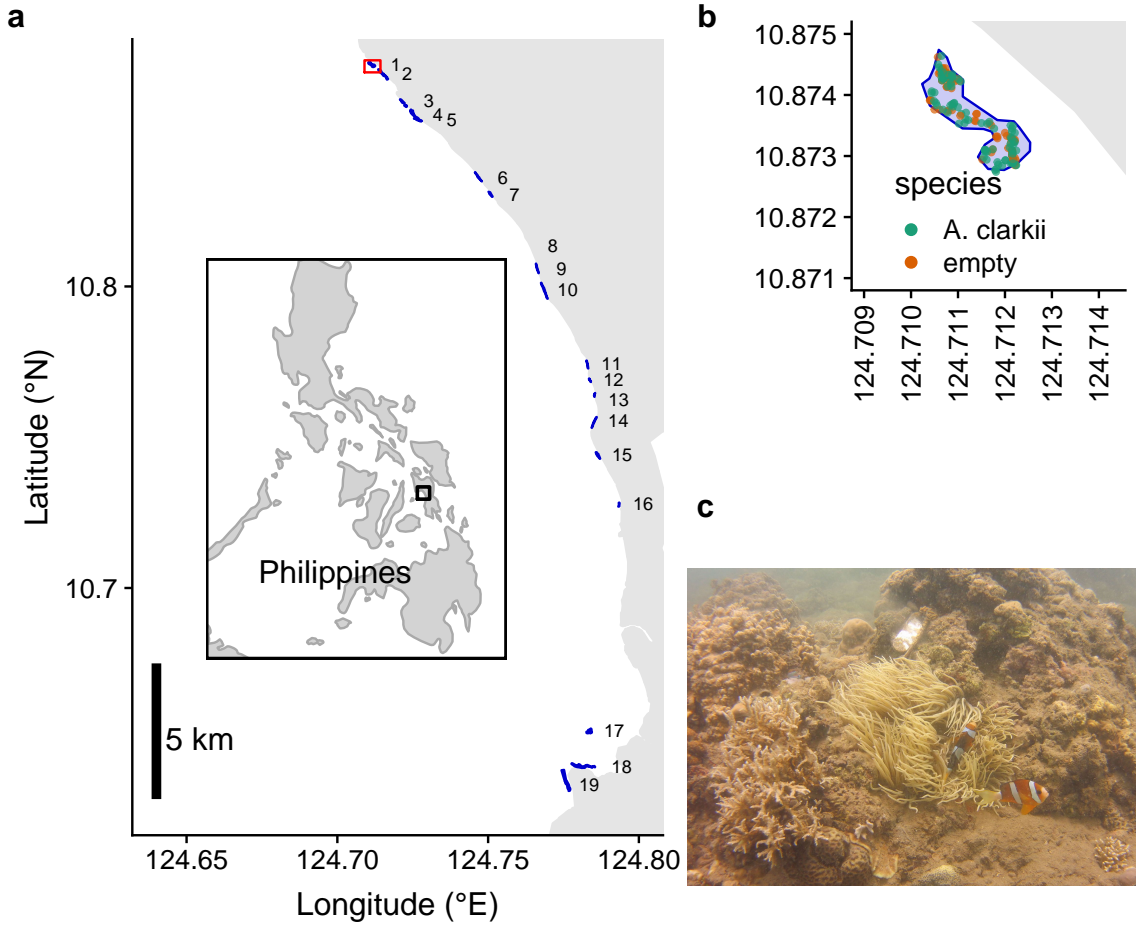


Figure 1: a) Map of the patches along the coast of Leyte in the Philippines. From north to south, the patches are: 1) Palanas, 2) Wangag, 3) North Magbangon, 4) South Magbangon, 5) Cabatoan, 6) Caridad Cemetery, 7) Caridad Proper, 8) Hicgop South, 9) Sitio Tugas, 10) Elementary School, 11) Sitio Lonas, 12) San Agustin, 13) Poroc San Flower, 14) Poroc Rose, 15) Visca, 16) Gabas, 17) Tomakin Dako, 18) Haina, and 19) Sitio Baybayon. b) Zoomed-in map of the northern-most patch, Palanas, to show anemone arrangement with anemones colored as occupied by *A. clarkii* (green) or unoccupied by anemonefish (orange). c) An example anemone occupied by *A. clarkii* in a typical habitat at the patches. The metal anemone tag is visible just above the anemone on the rock.

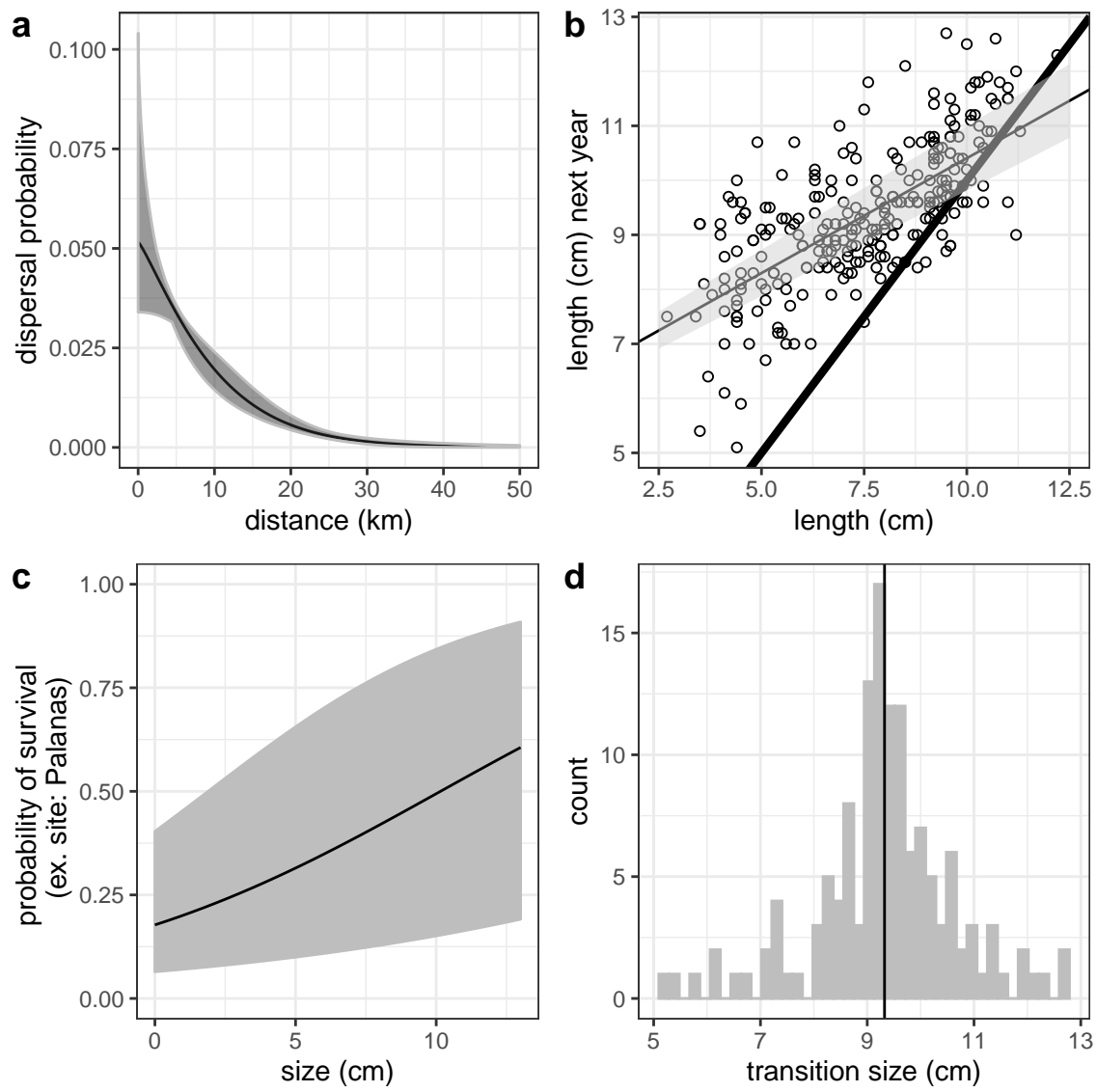


Figure 2: Best estimates (solid black line) and uncertainty (grey) for a) dispersal, b), growth, including the 1:1 line in thick black, c) post-recruit annual survival at Palanas as an example patch, and d) size at female transition parameters.

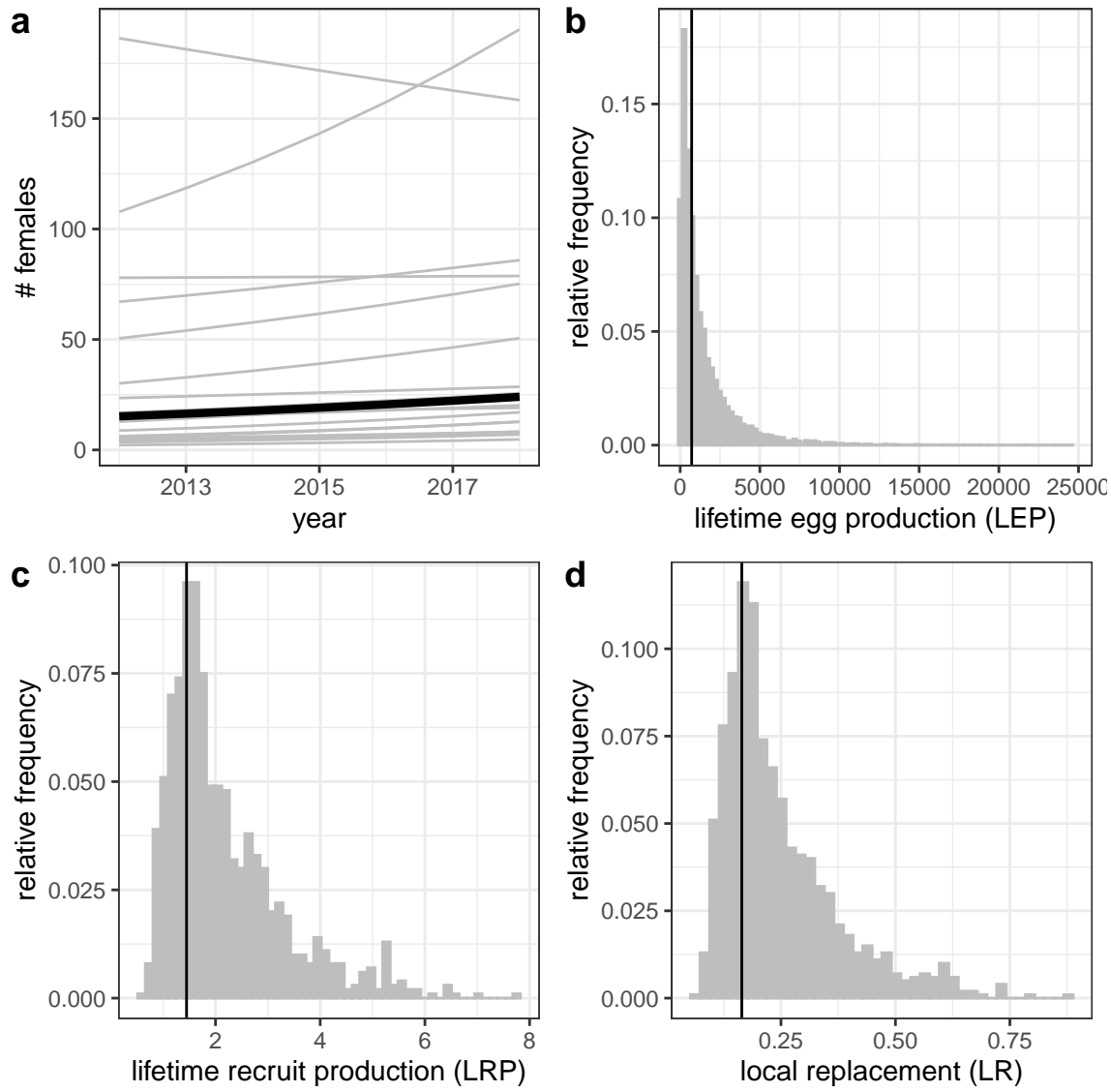


Figure 3: Estimates of a) estimated abundance of females over time at each individual patch (grey lines) and for an average patch (black line), b) individual-patch  $LEP_i$  for all patches with the best estimate averaged across patches (black line), c) average LRP across patches, and d) local replacement, showing the best estimate (black solid line) and range of estimates considering uncertainty in the inputs (grey). Estimates of LRP and LR include compensation for density-dependent mortality in early life stages.

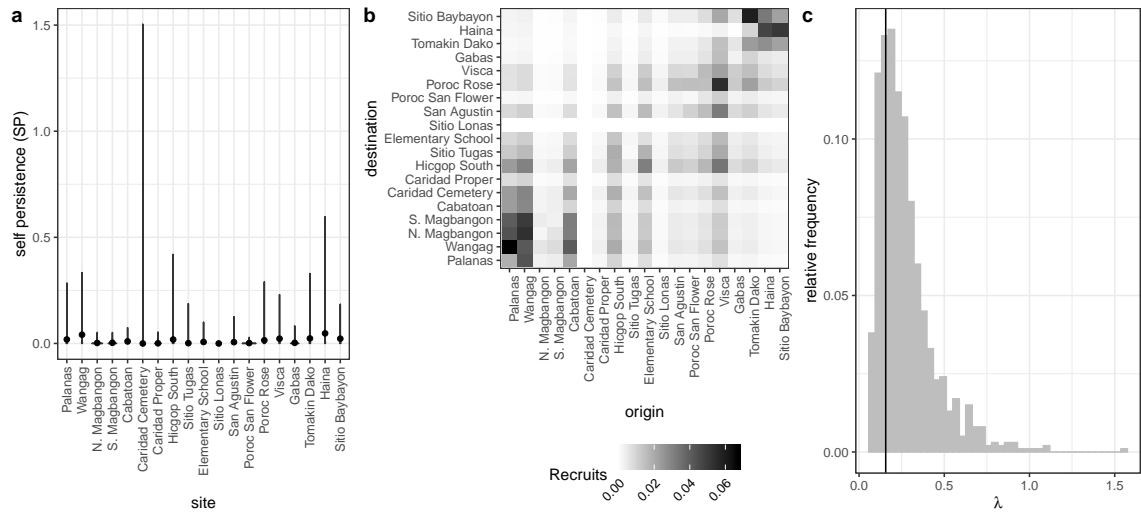


Figure 4: Values of a) self-persistence, b) realized connectivity among patches, and c) network persistence. All estimates include compensation for density-dependence in early life stages. For self-persistence (a) and network persistence (c), the best estimate is shown with in black (point for (a), line for (c)) and the range of estimates considering uncertainty is shown in grey.

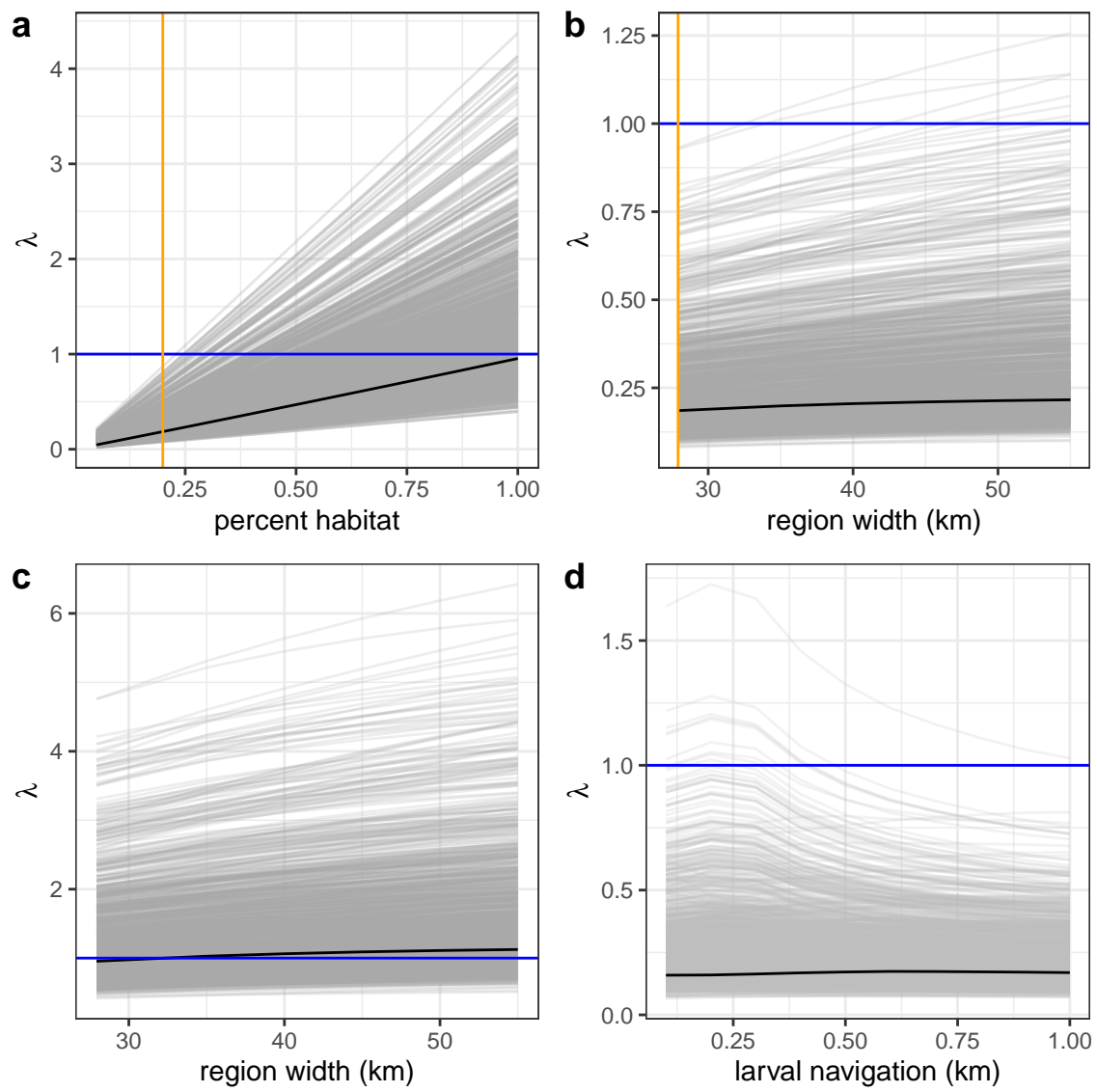


Figure 5: Sensitivity of network persistence to a) the proportion of the sampling region that is habitat, b) the width of the region maintaining the same proportion habitat (20%), c) the width of the region when 100% of the region is habitat, and d) larval navigation, where a buffer is added to the patch edges.

# Appendix

## A Supplemental Methods

### A.1 Defining recruit and census stage

When assessing persistence, we must consider mortality and reproduction that occurs across the entire life cycle to determine whether an individual is replacing itself with an individual that reaches the same life stage (Burgess et al., 2014). We defined a recruit to be a juvenile individual that has settled on the reef within the previous year, which also encompasses the size we were first able to sample (3.5-6.0 cm for parentage studies) (Fig. D.1). In theory, it does not matter how we defined recruit as long as we used that definition in our calculations of both egg-recruit survival and LEP. In our system, however, while it is straightforward to calculate LEP from any size, we did not have enough tagged recruits to reliably estimate survival to different recruit sizes. Instead, we chose the mean size of offspring matched in the parentage study as our best estimate of the size of a recruit ( $\text{size}_{\text{recruit}}$ ) and tested sensitivity to different recruit sizes by sampling from a uniform distribution over the sizes the recruit stage covers (3.5-6 cm, Table A1).

### A.2 Fecundity

We used a size-dependent fecundity relationship determined using photos of egg clutches and females (Yawdoszyn, in prep), where the number of eggs per clutch ( $E_c$ ) is exponentially related to the length in cm of the female ( $L$ ) with size effect

$\beta_l = 2.388$ , intercept  $b = 1.174$ , and egg age effect  $\beta_e = -0.608$  dependent on if the eggs were old enough to have visible eyes. We multiplied the number of eyed eggs per clutch by the number of clutches per year  $c_e = 11.9$  (estimate from Holtswarth et al., 2017) to get total annual fecundity  $f$  for a female of length  $L$ :

$$f = c_e * e^{\beta_l \ln(L) + \beta_e [\text{eyed}] + b}. \quad (\text{A.1})$$

### A.3 Growth and survival

To include size in the mark-recapture model for survival, we used the growth model (eqn. 6) and the size recorded or estimated in the previous year to estimate the size of fish not recaptured in a particular year. Fish are not well-mixed at our patches and divers needed to swim near an anemone to have a reasonable chance of capturing the fish on it so we also included a distance effect on recapture probability (Table A2). We used diver GPS tracks to estimate the minimum distance between a diver and the anemone where the fish was first caught for each tagged fish in each sample year.

We compared the fit of the models using a modified version of the Akaike information criterion that reduces the potential for overfitting with small sample sizes (AICc) and selected the model with the lowest AICc value (Table A2).

### A.4 LEP

To compute LEP, we discretized time and size (in eqn. 7) and summed across the matrix. When entering the starting individual into the matrix, we used 0.1 as the

standard deviation of size to spread out the starting individual across size bins. To account for differences in growth rates across fish, we used the size determined by the growth curve (eqn. 6) as the mean along with an estimate of spread ( $\text{size}_{sd}$ ) when projecting the size distribution of the fish in the next year. We used our recapture data to estimate the standard deviation ( $\text{size}_{sd}$ ) of the distribution of sizes in the next year of fish starting from one size (Table A1).

## A.5 Scaling up recruits

To estimate the total number of offspring produced by genotyped parents that survived to recruitment, we scaled up the number of matched offspring caught during sampling ( $R_m$ ) to account for recruits we could have missed (Fig. D.2). We scaled up by 1) the cumulative proportion of habitat we sampled at our patches over time ( $P_h$ ) to account for recruits at anemones we did not sample (details in A.6), 2) the probability of capturing a fish if we sampled its anemone ( $P_c$ ) to account for fish that escaped during sampling (details in A.7), 3) the proportion of the dispersal kernel from our patches covered within our sampling region ( $P_d$ ) to account for fish that dispersed outside of our sampling area (details in A.8), and 4) the proportion of our sampling region that was habitat ( $P_s$ ) to avoid counting mortality of fish dispersing to non-habitat within our region twice (in both the estimate of total recruits and in the integrated dispersal kernel) (details in A.9).

## A.6 Proportion of habitat sampled

We used tagged anemones to estimate the proportion of habitat we sampled within our patches. We tagged each anemone that was home to yellowtail anemonefish with a metal tag, which is relatively permanent and easy to re-sight (the anemone tag is visible above the anemone in Fig. 1c). We therefore considered the total number of metal-tagged anemones at a patch to be the habitat present. We used proportion of anemones rather than proportion of total patch area because anemones, and therefore habitat quality, were unevenly distributed across each patch; areas we did not visit likely had a lower anemone density than the areas we did sample.

To scale the number of tagged recruited offspring to account for areas of our patches we did not sample, we used the overall proportion habitat sampled across all patches and sampling years ( $P_h$ ). We summed the metal-tagged anemones we visited across all patches and years, then divided by the number of anemones we could have sampled (the sum of total metal-tagged anemones across all patches multiplied by the number of sampling years).

## A.7 Probability of capturing a fish, from recapture dives

To estimate the probability of capturing a fish given that we sampled its anemone ( $P_c$ ), we used mark-recapture data from recapture dives done within a sampling season. During some of the sampling years, portions of the patches were sampled again within a few weeks of the original sampling dives. We assumed that the probability of recapturing a fish on a recapture dive was the same as capturing a fish

on a sampling dive, assuming there was no mortality in the weeks between dives and that the fish did not alter their behavior towards divers. For each recapture dive, we used GPS tracks of the divers to identify the anemones covered in the recapture dive and the set of PIT-tagged fish encountered on those anemones during the original sampling dives. We estimated the probability of capture  $P_c$  as the number of tagged fish re-caught during the capture dive  $m_2$  divided by the total number of fish caught on the recapture dive  $n_2$ :  $P_c = \frac{m_2}{n_2}$ .

We used the mean  $P_c$  across all 14 recapture dives, covering XX patches in 3 sampling seasons (2016, 2017, 2018), as our best estimate. To consider uncertainty in  $P_c$ , we represented the probability of capture as a beta distribution, using the mean  $\mu_{P_c}$  and variance  $V_{P_c}$  of the set of 14 values to find the appropriate  $\alpha_{P_c}$  and  $\beta_{P_c}$  parameters, where

$$\alpha_{P_c} = \left( \frac{1 - \mu_{P_c}}{V_{P_c}} - \frac{1}{\mu_{P_c}} \right) \mu_{P_c}^2 \quad (\text{A.2})$$

$$\beta_{P_c} = \alpha_{\mu_{P_c}} \times \frac{1}{\mu_{P_c} - 1}. \quad (\text{A.3})$$

The mean of the individual capture probability values was  $\mu_{P_c} = 0.56$ , with variance  $V_{P_c} = 0.069$ , giving beta distribution parameters  $\alpha_{P_c} = 1.44$  and  $\beta_{P_c} = 1.13$ . We sampled 1000 values from the beta distribution, then truncated the sample to include only values larger than the lowest value of  $P_c$  estimated from an individual dive (0.20), to avoid unrealistically low values randomly sampled from the distribution. We then sampled with replacement from the truncated set to get a vector of

1000 values.

## A.8 Proportion of dispersal kernel area sampled

To account for recruits that dispersed outside our sampling region, we found the proportion of the dispersal kernels from all parents that fell within our sampling region. For each of the nineteen patches, we found the area under the kernel ( $A_i$ ) from the center of the patch to the north edge of the sampling area ( $d_N$ ) (northern-most tagged anemone at Palanas, the northern-most patch) and the center of the patch to the south edge of the sampling area ( $d_S$ ) (southern-most tagged anemone at Sitio Baybayon, the southern-most patch), then multiplied by the number of genotyped parents at that patch ( $N_{g_i}$ ). We added the areas together, then divided by the sum of the total area under the dispersal kernel in both directions (1 when the kernel was normalized to 0.5) multiplied by the total number of genotyped parents ( $N_g$ ) to get the proportion of the total dispersal kernel area covered by our sampling region ( $P_d$ ):

$$A_i = N_{g_i} \left( \int_0^{d_N} z e^{-(zd)^{\theta}} dd + \int_0^{d_S} z e^{-(zd)^{\theta}} dd \right), \quad (\text{A.4})$$

$$P_d = \frac{\sum_{i=1}^{19} A_i}{N_g}. \quad (\text{A.5})$$

## A.9 Proportion habitat in sampling area

To avoid counting mortality due to larvae settling on non-habitat twice - once in scaling up our matched recruits, which only included those who settled on habitat, and once in integrating the dispersal kernel - we scaled the estimate of total surviving recruits from our patches by the proportion of our sampling region that was habitat ( $P_s$ ). We found  $P_s$  by summing the lengths of all the patches, which run approximately north-south, and dividing by the total north-south distance of our sampling region, giving  $P_s = 0.20$ . We assumed that larvae were unable to navigate to habitat if they dispersed to an unsuitable area but relaxed that assumption in our sensitivity tests (A.10.0.1) as anemonefish larvae do likely have some ability both to sense good settlement areas, either by detecting host anemones (Elliott et al., 1995; Arvedlund et al., 1999) or conspecifics (e.g. Lecchini et al., 2005, for coral reef fish more broadly), and to swim in a particular direction (e.g. Bellwood and Fisher, 2001; Fisher, 2005).

## A.10 Sensitivity tests

### A.10.0.1 Larval navigation

In our sensitivity test to larval navigation and swimming, we added a buffer representing navigation ranging from 0 - 1 km to the edges of the destination patches when determining probability of dispersal between patches. To avoid the shadows of effective patch area from overlapping, we added no more than half the distance between two adjacent patches to each patch. The buffers changed the proportion of

the sampling region that is habitat (A.9), as we considered the buffer areas to be habitat as well, which affected the scaling of recruits in egg-recruit survival.

## A.11 Characterizing uncertainty

### A.11.0.1 Size of transition to female

To incorporate uncertainty in the size at which male fish transition to female (and reproductive output is counted in eqn. 7), we sampled directly from the sizes at which recaptured fish were first captured as female (5.2 cm - 12.7 cm) (Fig. 2d).

### A.11.0.2 Egg-recruit survival

We considered uncertainty in the number of offspring assigned to parents ( $R_m$ ) and in the probability of capturing a fish ( $P_c$ ). We generated a set of values for the number of assigned offspring using a random binomial, with the number of genotyped offspring (745) as the number of trials and the assignment rate from the parentage analysis (0.079) as the probability of success on each trial (Catalano et al., in prep). For the probability of capturing a fish, we sampled values from a beta distribution that captured the mean and variance of capture probabilities across recapture dives (details in A.3).

### A.11.0.3 Dispersal kernel

To account for uncertainty in the dispersal kernel, we used sets of the shape parameter  $\theta$  and the scale parameter  $k_d$  that represented the span of the 95% confidence interval when  $k_d$  and  $\theta$  were estimated jointly (Table A1, Catalano et al., in prep).

## B Supplemental Results

### B.1 Growth

From the mark-recapture analysis of tagged and genotyped fish, we estimated mean values of  $L_\infty = 10.70$  cm (with 95% confidence intervals 9.81-11.65) and  $K = 0.864$  (0.80-0.91) for the von Bertalanffy growth curve parameters (eqn. 6, Fig. 2b, Table A1).

### B.2 Survival

The best model for post-recruitment annual survival  $\phi$  on a log-odds scale had a positive size effect ( $b_a = 0.15 \pm 0.029$  SE) with intercepts  $b_{\phi_i}$  varying by patch (eqn. B.1, Fig. D.5). The accompanying best model for recapture probability  $p_r$  on a log-odds scale had a negative effect of size ( $b_1 = -0.16 \pm 0.09$  SE) and a negative effect of diver distance from anemone ( $b_2 = -0.15 \pm 0.02$  SE), with intercept  $b_{p_r} = 2.14 \pm 0.87$  SE (eqn. B.2, Fig. D.6). This suggests divers were less likely to recapture larger fish, which are stronger swimmers and more likely to flee when divers approach, and those at anemones far from areas sampled:

$$\log\left(\frac{\phi}{1-\phi}\right) = b_{\phi_i} + b_a \text{size}. \quad (\text{B.1})$$

$$\log\left(\frac{p_r}{1-p_r}\right) = b_{p_r} + b_1 \text{size} + b_2 d. \quad (\text{B.2})$$

### B.3 Lifetime egg production (LEP)

We calculated an average value of LEP across patches of 721 eggs [82, 31657] (Fig. 3b), with best estimate values at individual patches that ranged from 0 to 1754 eggs. Uncertainty in adult survival had the largest effect on LEP (Fig. D.10), which corresponds to longer-surviving individuals having more opportunities to reproduce at larger sizes.

### B.4 Egg-recruit survival ( $S_e$ )

We estimated egg-recruit survival  $S_e$  to be 0.002 [3.5e-05, 0.014] when we corrected for density-dependence in our data. Uncertainty in the size of transition to breeding female  $L_f$  had the largest effect on egg-recruit survival (Fig. D.12); the larger the transition size to female, the fewer tagged eggs we estimated were produced by our genotyped parents and the higher the estimate of egg-recruit survival. This differs from our finding above that adult survival had the largest effect on LEP because the starting size of the individual considered is lower when we estimate LEP for a recruit (4.37 cm, 3.5-6.0cm range) than for a parent (6.0cm). Fish considered parents in our parentage analysis have already survived one or more years since recruiting so the transition to breeding female plays a larger role in the number of eggs they are likely to produce than for fish who have just recruited.

### B.5 Abundance trends by patch

We used the number of females captured at each patch in each sampling year, scaled by the proportion of habitat sampled at that patch in that year and by the prob-

ability of capturing a fish, to estimate abundance trends for each patch (Fig. D.7). Seventeen of the patches showed positive abundance trends (Fig. D.7a-q), while the two southern-most patches showed declines (Haina and Sitio Baybayon, Fig. D.7r,s).

## B.6 Persistence metrics without compensation for density-dependence

Estimating persistence metrics without compensating for density-dependence in our data gave us an understanding of whether individuals at our patches were able to replace themselves and whether our patches would persist in isolation at the current abundance levels, rather than at low abundance. Without compensation for early life density-dependence, all of our metrics showed that the set of patches we sampled is less likely to persist as an isolated network than the metrics for low abundance. We estimated egg-recruit survival ( $S_e$ ) to be 0.0012 [2.04e-05, 0.008] and average lifetime recruit production (LRP) across patches to be 0.84 [0.36, 4.54], with 55% of LRP estimates  $\geq 1$ . (Fig. D.8c). Our estimate of local replacement (LR), which estimates replacement for recruits from our patches returning to our patches implicitly including dispersal, was 0.10 [0.04, 0.52].

When we calculated LR using all arriving recruits to our patches, however, rather than just those originating there, the best estimate was  $> 1$  (1.22, with 89% of values with uncertainty  $\geq 1$ ), suggesting that there was recruit-recruit replacement at our patches when we included immigrant recruits, even at current population levels when density-dependence was present.

We did not find any patches with a best estimate or uncertainty range of SP  $\geq 1$

Figs. D.9a). Our best estimate of the dominant eigenvalue of the realized connectivity matrix  $\lambda_c$  was 0.09 [0.04, 0.90] with 0% of estimates where  $\lambda \geq 1$  (Fig. D.9c).

## C Supplemental Tables

Table A1: Summary of parameter symbols, definitions, and values.

Parameter	Description	Best estimate	Range in uncertainty runs	Notes
$k_d$	scale parameter in dispersal kernel	-2.33	-2.81 to -1.22	eqn. 5, estimated using methods in Bode et al. (2018) in Catalano et al. (in prep)
$\theta$	shape parameter in dispersal kernel	1.19	0.63 to 2.04	eqn. 5, estimated using methods in Bode et al. (2018) in Catalano et al. (in prep)
$L_\infty$	average asymptotic size (cm) in von Bertalanffy growth curve	10.70 cm	9.81 to 11.65 cm	eqn. 6
$K$	growth coefficient in von Bertalanffy growth curve	0.864	0.80 to 0.91	eqn. 6

$b_{\phi_{Cabatoan}}$	intercept for adult survival at 0 cm at Cabatoan	-1.78	$\pm 0.33$ standard error	on a log-odds scale, eqn. B.1
$i_{\phi_{Cardidad Cemetery}}$	addition to intercept for survival at Caridad Cemetery	-19.61	$\pm 2994$ standard error	on a log-odds scale, eqn. B.1
$i_{\phi_{Elementary School}}$	addition to intercept for survival at Elementary School	-0.11	$\pm 0.41$ standard error	on a log-odds scale, eqn. B.1
$i_{\phi_{Gabas}}$	addition to intercept for survival at Gabas	-0.42	$\pm 0.58$ standard error	on a log-odds scale, eqn. B.1
$i_{\phi_{Haina}}$	addition to intercept for survival at Haina	0.12	$\pm 0.35$ standard error	on a log-odds scale, eqn. B.1
$i_{\phi_{Hicgop South}}$	addition to intercept for survival at Hicgop South	-0.06	$\pm 0.46$ standard error	on a log-odds scale, eqn. B.1

$i_{\phi_{N.Magbangon}}$	addition to intercept for survival at N. Magbangon	-1.31	$\pm$ 0.38 standard error	on a log-odds scale, eqn. B.1
$i_{\phi_{Palanas}}$	addition to intercept for survival at Palanas	0.24	$\pm$ 0.26 standard error	on a log-odds scale, eqn. B.1
$i_{\phi_{PorocRose}}$	addition to intercept for survival at Poroc Rose	-0.19	$\pm$ 0.44 standard error	on a log-odds scale, eqn. B.1
$i_{\phi_{PorocSanFlower}}$	addition to intercept for survival at Poroc San Flower	-0.52	$\pm$ 0.48 standard error	on a log-odds scale, eqn. B.1
$i_{\phi_{SanAgustin}}$	addition to intercept for survival at San Agustin	-0.47	$\pm$ 0.50 standard error	on a log-odds scale, eqn. B.1
$i_{\phi_{SitioBaybayon}}$	addition to intercept for survival at Sitio Baybayon	0.02	$\pm$ 0.26 standard error	on a log-odds scale, eqn. B.1

$i_{\phi_{S.Magbangon}}$	addition to intercept for survival at S. Magbangon	-1.08	$\pm$ 0.48 standard error	on a log-odds scale, eqn. B.1
$i_{\phi_{TomakinDako}}$	addition to intercept for survival at Tomakin Dako	0.39	$\pm$ 0.33 standard error	on a log-odds scale, eqn. B.1
$i_{\phi_{Visca}}$	addition to intercept for survival at Visca	0.33	$\pm$ 0.35 standard error	on a log-odds scale, eqn. B.1
$i_{\phi_{Wangag}}$	addition to intercept for survival at Wangag	0.35	$\pm$ 0.25 standard error	on a log-odds scale, eqn. B.1
$b_a$	size effect for adult survival	0.15	$\pm$ 0.03 standard error	on a log-odds scale, eqn. B.1
$\beta_e$	coefficient for eyed eggs	-0.608		eqn. A.1, Yawdoszyn et al. (in prep)
$\beta_l$	size effect in eggs-per-clutch relationship	2.39		eqn. A.1, Yawdoszyn et al. (in prep)

$b$	intercept in eggs-per-clutch relationship at female size 0 cm	1.17		eqn. A.1, Yawdoszyn et al. (in prep)
$c_e$	egg clutches per year	11.9		eqn. A.1, Holtswarth et al. (2017)
$\text{size}_{\text{recruit}}$	size (cm) of recruited offspring	mean of size of offspring in parentage analysis = 4.37 cm	3.5 - 6.0 cm	drawn from uniform distribution across range
$\text{size}_{\text{recruit},sd}$	standard deviation of size of a recruit	0.1		used in discretization of IPM for LEP
$\text{size}_{sd}$	standard deviation distribution of sizes of a fish in the next year	1.45		used in discretization of IPM for LEP, estimated from range of sizes for fish starting at 7.4-7.6 cm and recaptured a year later

$L_s$	minimum size in LEP IPM	0 cm		eqn. 7
$U_s$	maximum size in LEP IPM	15 cm		eqn. 7
$L_f$	size at transition to female	9.32 cm	5.2 - 12.7 cm	drawn from distribu- tion in data
$R_m$	number of off- spring matched to parents	62 offspring		eqn. 8
$N_g$	number of geno- typed parents	1719 fish		eqn. 8
$P_h$	proportion of patches sampled cumulatively across time	0.41		eqn. 8, details in A.6
$P_d$	proportion of dispersal kernel area from each patch covered by our sampling region	0.57		eqn. 8, details in A.8

$P_c$	probability of capturing a fish	0.56	drawn from beta distribution with parameters $\alpha_{P_c} = 1.44$ and $\beta_{P_c} = 1.13$	eqn. 8, details in A.7
$P_s$	proportion of our sampling region that is habitat	0.20		eqn. 8, details in A.9
DD	proportion of habitat that would be available without density-dependence at settlement	1.71		eqn. 8
$p_U$	proportion of anemones unoccupied by clownfish	0.53		used to estimate DD

$p_A$	proportion of anemones occupied by $A.$ <i>clarkii</i>	0.38		used to estimate DD
-------	---	------	--	---------------------

Table A2: Table showing the set of models considered in MARK for survival ( $\phi$ ) and recapture ( $p$ ) probability, including effects of size ( $S$ ), minimum distance from diver to anemone during surveys ( $D$ ), time ( $t$ ), and patch ( $i$ ), and their relative AICc scores.

Model	Model description	AICc	dAICc
$\phi \sim S + i, p \sim S + D$	survival size+patch, recapture size+distance	3104.1	0
$\phi \sim i, p \sim D$	survival patch, recapture size+distance	3127.1	23
$\phi \sim i, p \sim D$	survival patch, recapture distance	3127.2	23
$\phi \sim S, p \sim S + D$	survival size, recapture size+distance	3139.9	35.8
$\phi \sim S, p$	survival size, recapture distance	3141.6	37.5
$\phi, p \sim S + D$	survival constant, recapture size+distance	3168.3	64.2
$\phi, p \sim D$	survival constant, recapture distance	3169.3	65.2
$\phi \sim t, p$	survival time, recapture constant	3243.9	139.7
$\phi \sim i, p$	survival patch, recapture constant	3254.4	150.3
$\phi, p \sim t$	survival constant, recapture time	3274.0	169.9
$\phi \sim S, p \sim S$	survival size, recapture size	3345.2	241.0
$\phi, p$	survival constant, recapture constant	3382.7	278.5

Table A3: Table showing the percent of anemones surveyed at each patch, ordered from north to south, in each sampling year.

		% Habitat surveyed							
Patch	# Total anems	2012	2013	2014	2015	2016	2017	2018	
Palanas	137	29	58	47	63	85	86	86	
Wangag	296	18	32	42	34	26	49	68	
N. Magbangon	105	5	12	40	63	63	0	5	
S. Magbangon	34	41	56	32	0	65	0	71	
Cabatoan	26	42	58	58	65	73	0	62	
Caridad Cemetery	4	0	75	50	0	50	50	50	
Hicgop South	18	0	67	22	28	56	83	78	
Elementary School	8	0	100	38	88	88	88	100	
San Agustin	17	94	65	71	65	100	82	76	
Poroc San Flower	11	100	82	73	73	55	82	64	
Poroc Rose	13	100	100	69	31	23	69	69	
Visca	13	100	100	23	38	62	85	62	
Gabas	9	0	0	0	44	44	67	0	
Tomakin Dako	50	0	24	22	36	34	60	68	
Haina	104	0	6	13	13	10	56	80	
Sitio Baybaon	260	0	14	30	33	30	41	80	
Overall	1105	16	31	37	39	42	48	68	

## D Supplemental Figures

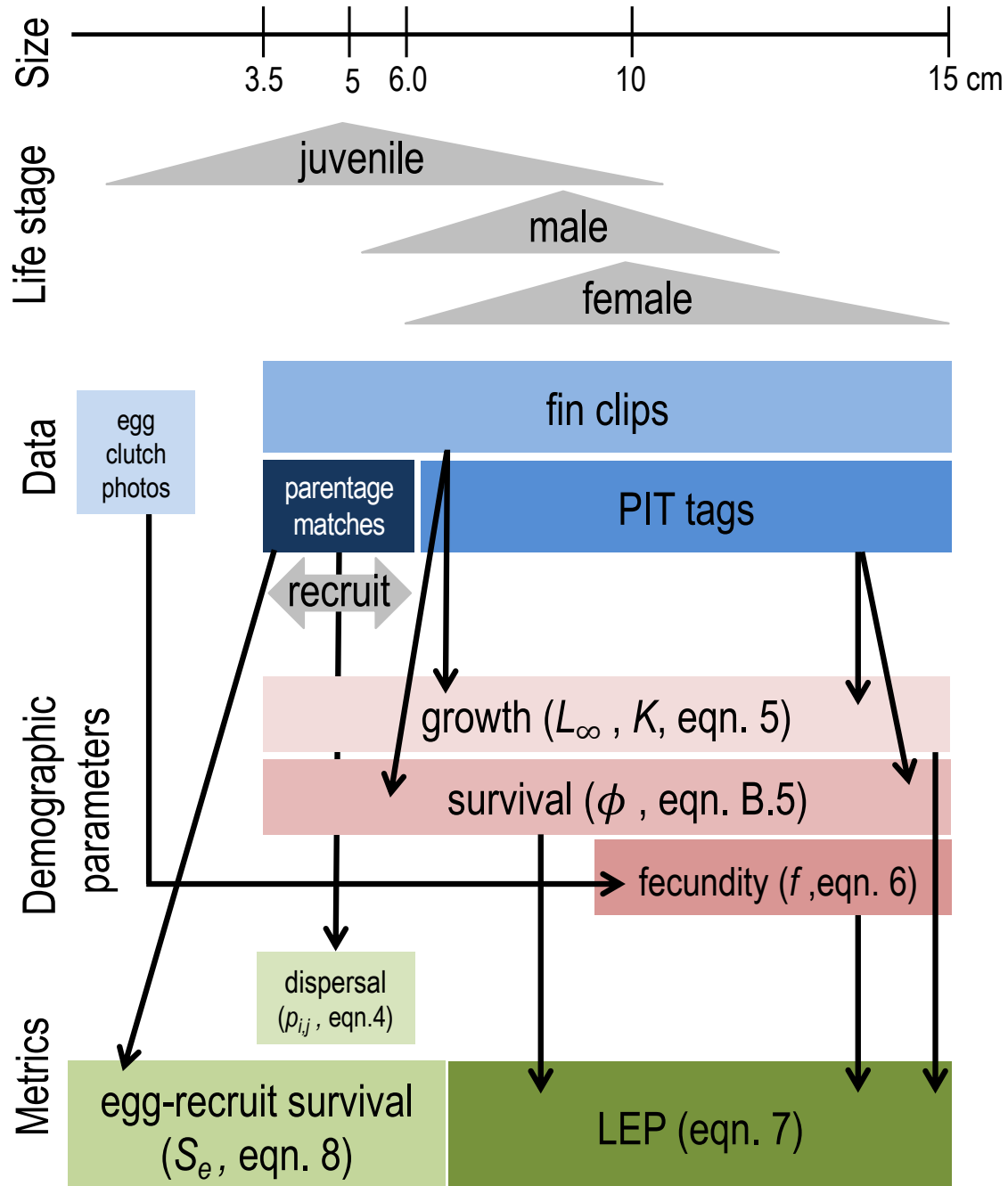


Figure D.1: The data collected for fish at each life stage and how they match to the equations and metrics estimated. We considered recruits to be offspring in their first year of settlement, represented by the 3.5–6.0 cm range.

## How could we have missed potential recruits originating from our patches?

- 1) Failed to catch recruit when sampling ( $P_c$ )
- 2) Missed sampling some habitat areas within our patches ( $P_h$ )
- 3) Recruit dispersed outside our study region ( $P_d$ )
- 4) Recruit dispersed to non-habitat within our region ( $P_s$ )
- 5) Recruit died due to density-dependent competition with other settlers (DD)

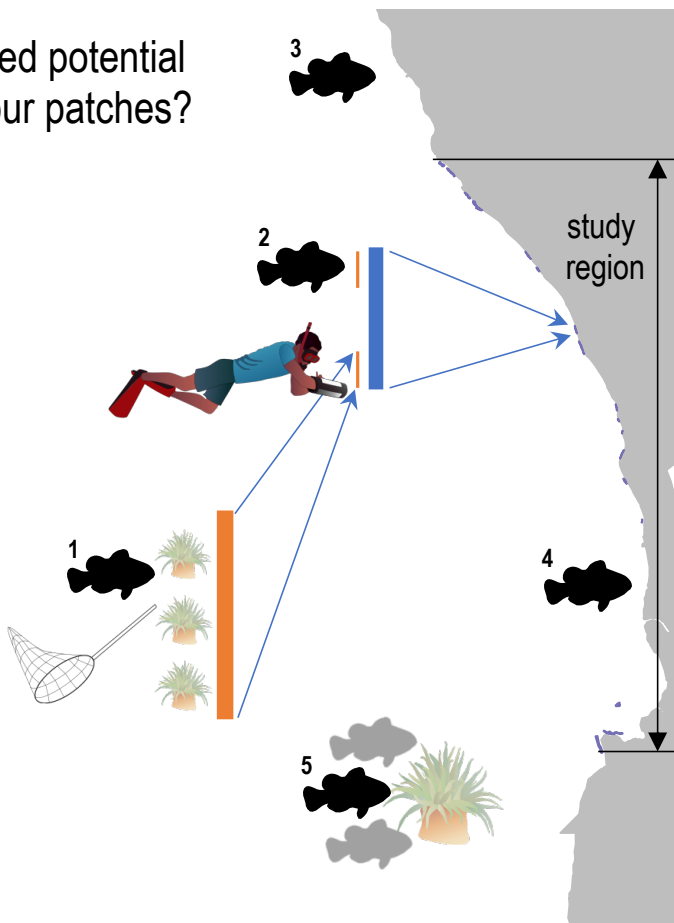


Figure D.2: Schematic of five ways we could have missed recruits while sampling and used to scale up our raw estimate of recruits from matched offspring.

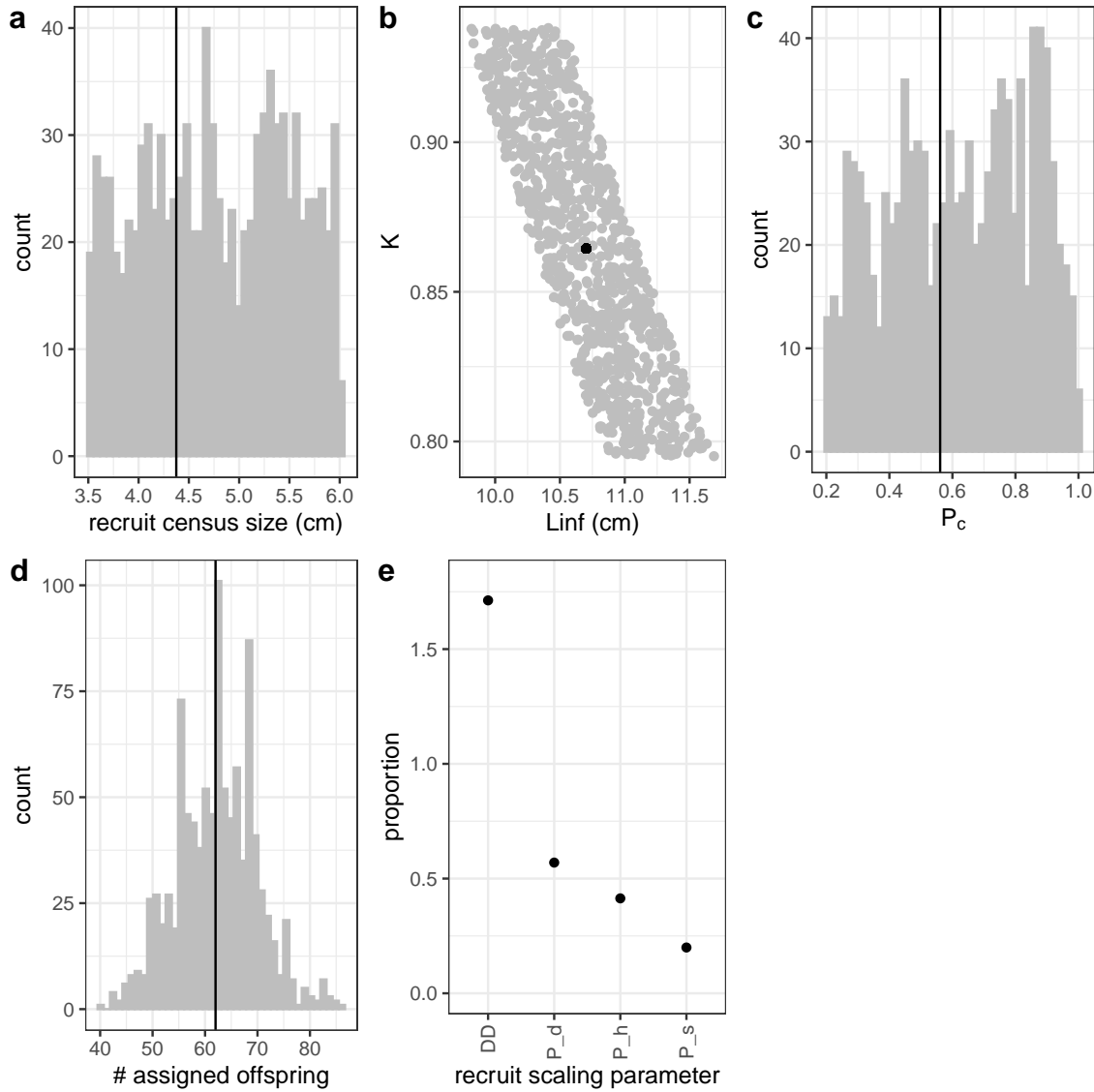


Figure D.3: Range of parameter inputs for uncertainty runs with all uncertainty included, where the black line or point is the value used for the best estimate: a)  $\text{size}_{\text{recruit}}$ , the census size for recruits after egg-recruit survival; b) the parameters  $L_\infty$  and  $K$  of the von Bertalanffy growth model; c)  $P_c$ , the probability of capturing a fish; d) number of offspring assigned back to parents in the parentage analysis; e) factors that scale the number of estimated recruits from our patch based on density-dependence in settler success (DD), proportion of the dispersal kernel captured by our sampling region ( $P_d$ ), the cumulative proportion of our patches we sampled over time ( $P_h$ ), and the proportion of our sampling area that was habitat ( $P_s$ ).

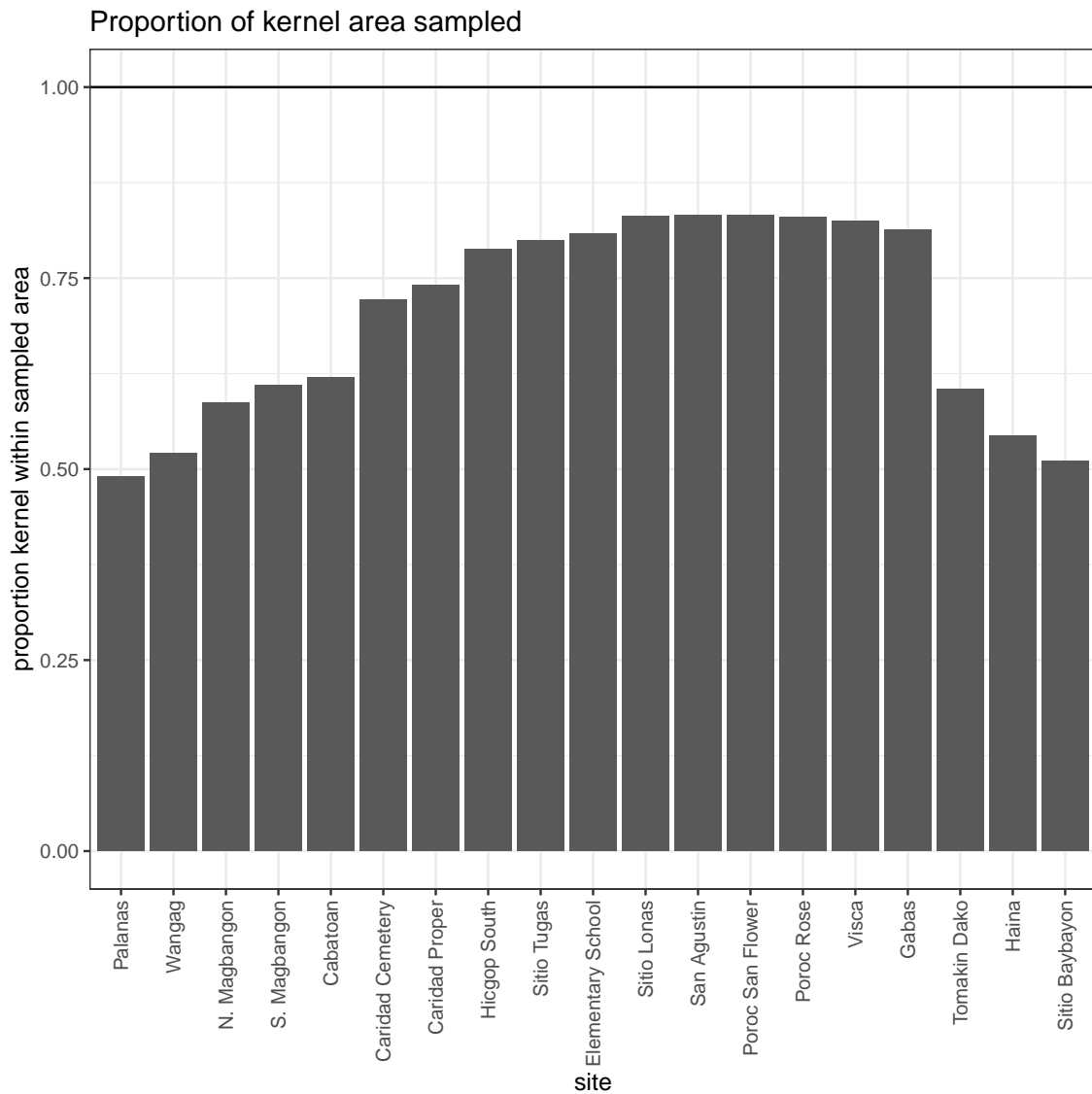


Figure D.4: Proportion of the dispersal kernel area from the center of each patch covered by our sampling region. The overall proportion ( $P_d$ ) is weighted by the number of parents at each patch.

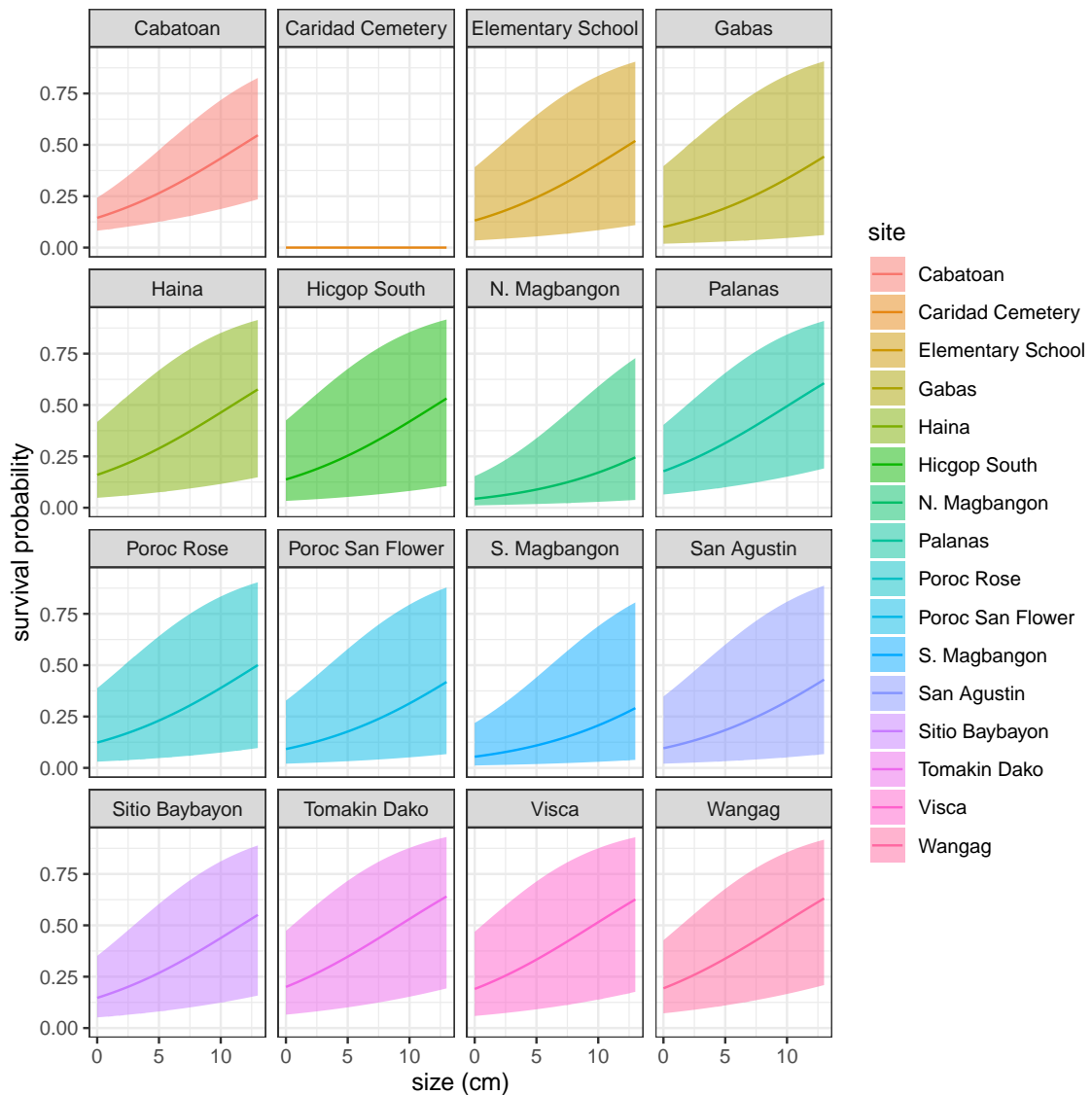


Figure D.5: Annual survival by size at each patch.

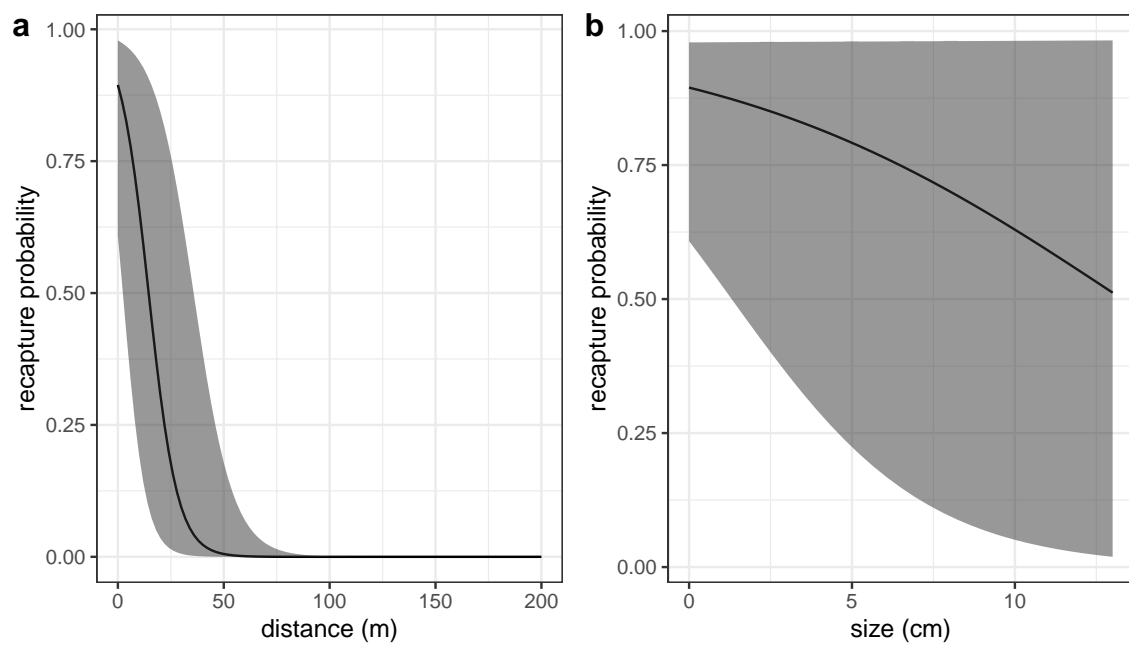


Figure D.6: Effects of a) minimum distance between divers and the anemone where the fish was first caught and b) fish size on recapture probability, estimated along with survival in a mark-recapture analysis.

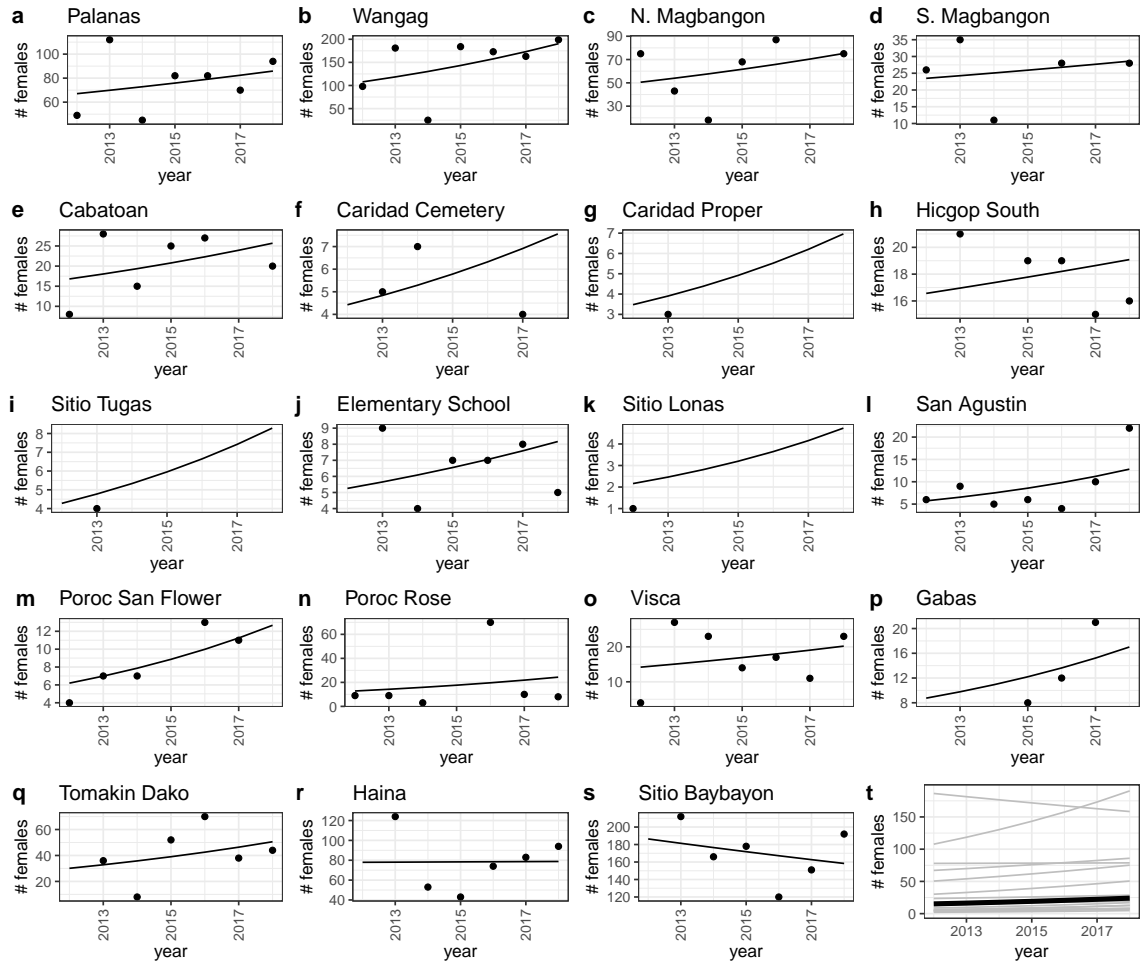


Figure D.7: Scaled number of females captured (black dots) and abundance trends (black lines) by patch from a mixed effects model with patch as a random effect.

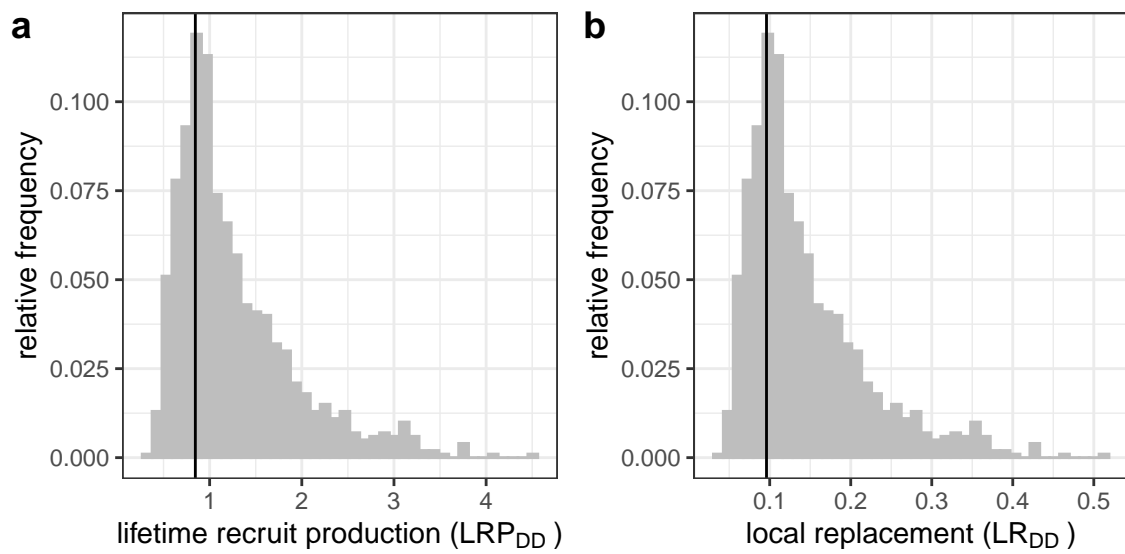


Figure D.8: Estimates of a) LRP, and b) local replacement without compensating for density dependence in early life stages in our data, showing the best estimate (black solid line) and range of estimates considering uncertainty (grey) in the inputs. These estimates compare to those in 3c,d, where we corrected for additional mortality in early life due to density dependence.

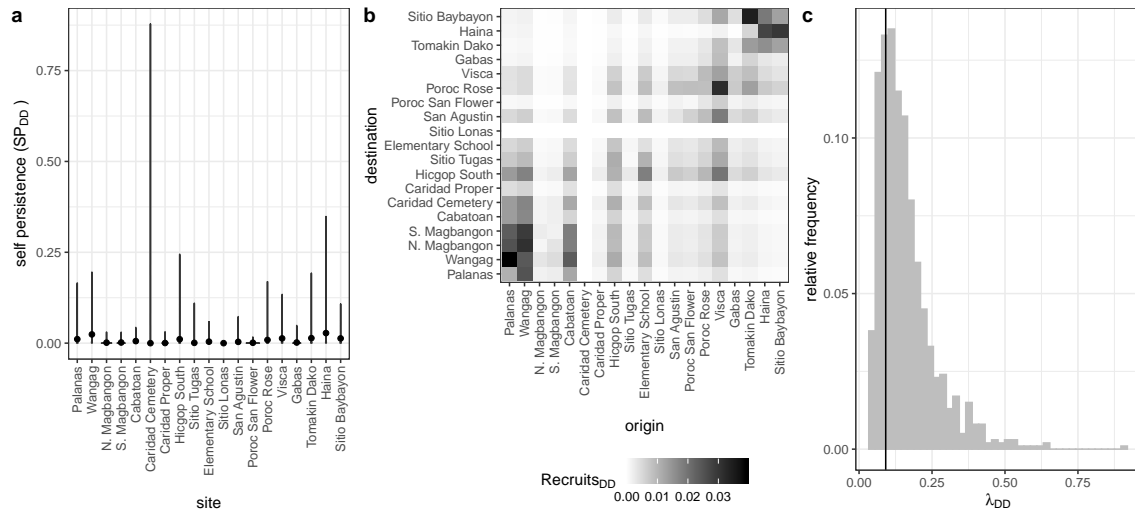


Figure D.9: Values of a) self-persistence, b) realized connectivity among patches, and c) network persistence without compensation for density-dependence in early life stages in our data. For self-persistence (a) and network persistence (c), the best estimate is shown with in black (point for (a), line for (c)) and the range of estimates considering uncertainty is shown in grey. These estimates compare to those in 4 where we compensated for density dependence in early life stages.

Here we show the contribution of uncertainty of each input to the overall uncertainty in the values of LEP (Fig. D.10), LRP (Fig. D.11), egg-recruit survival  $S_e$  (Fig. D.12), and network persistence  $\lambda_c$  (Fig. D.13). We calculated the metrics using best estimates for all inputs except the one shown and show the results as violin plots, which show vertical probability densities of the metrics across a range of values.

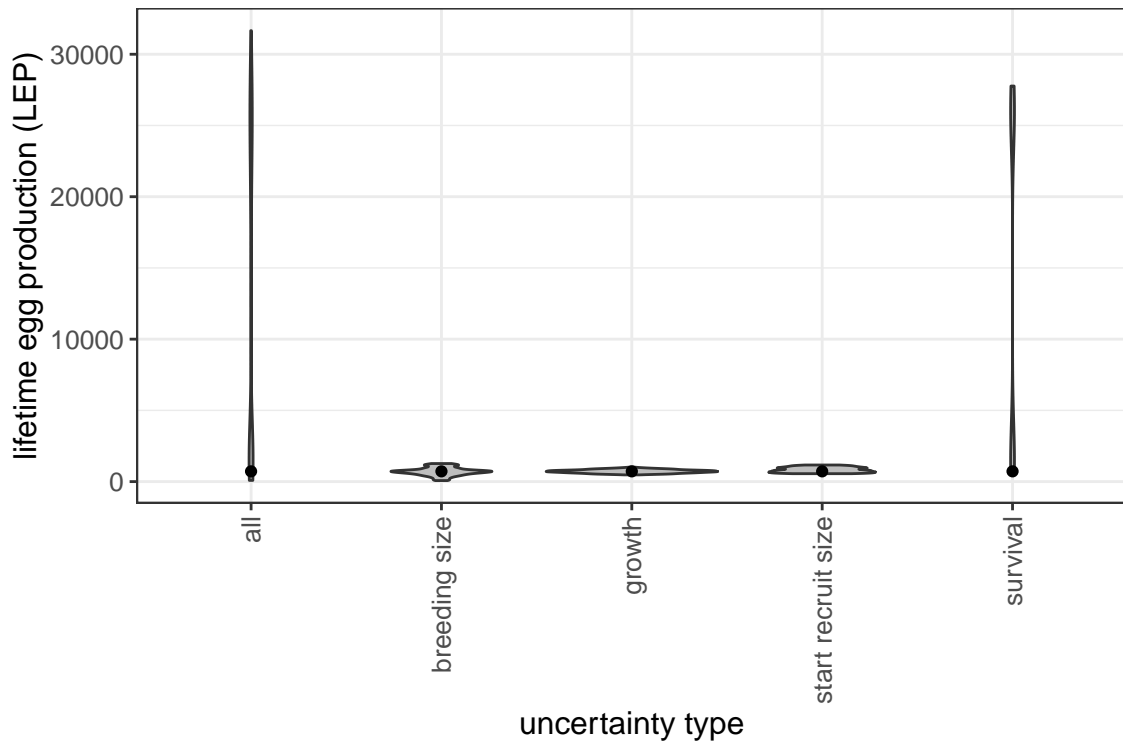


Figure D.10: The contribution of different sources of uncertainty in LEP.

## Comparison to other studies

### D.1 Persistence metrics

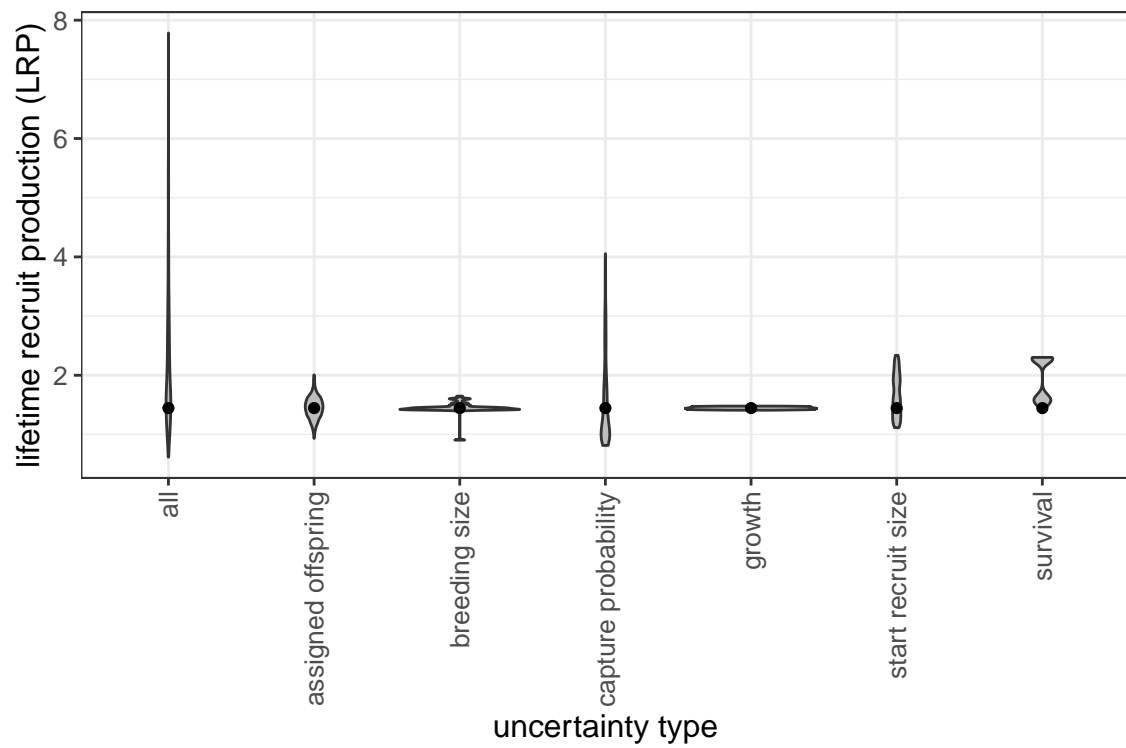


Figure D.11: The contribution of different sources of uncertainty in LRP.

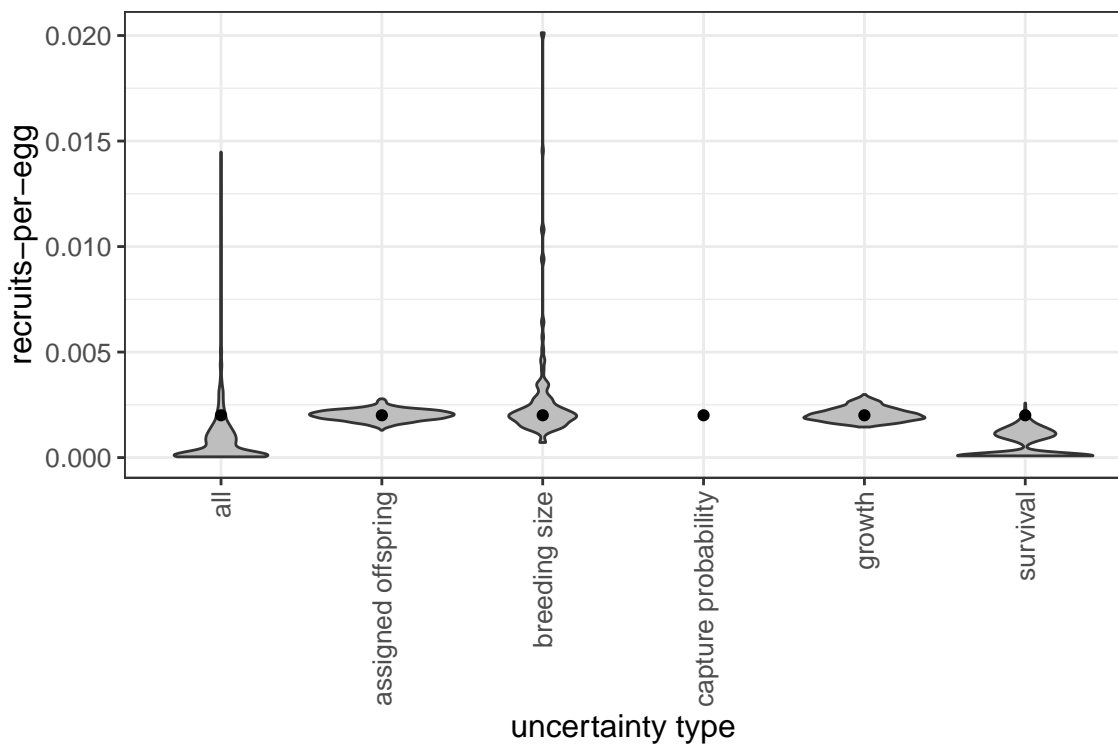


Figure D.12: The contribution of different sources of uncertainty in egg-recruit survival.

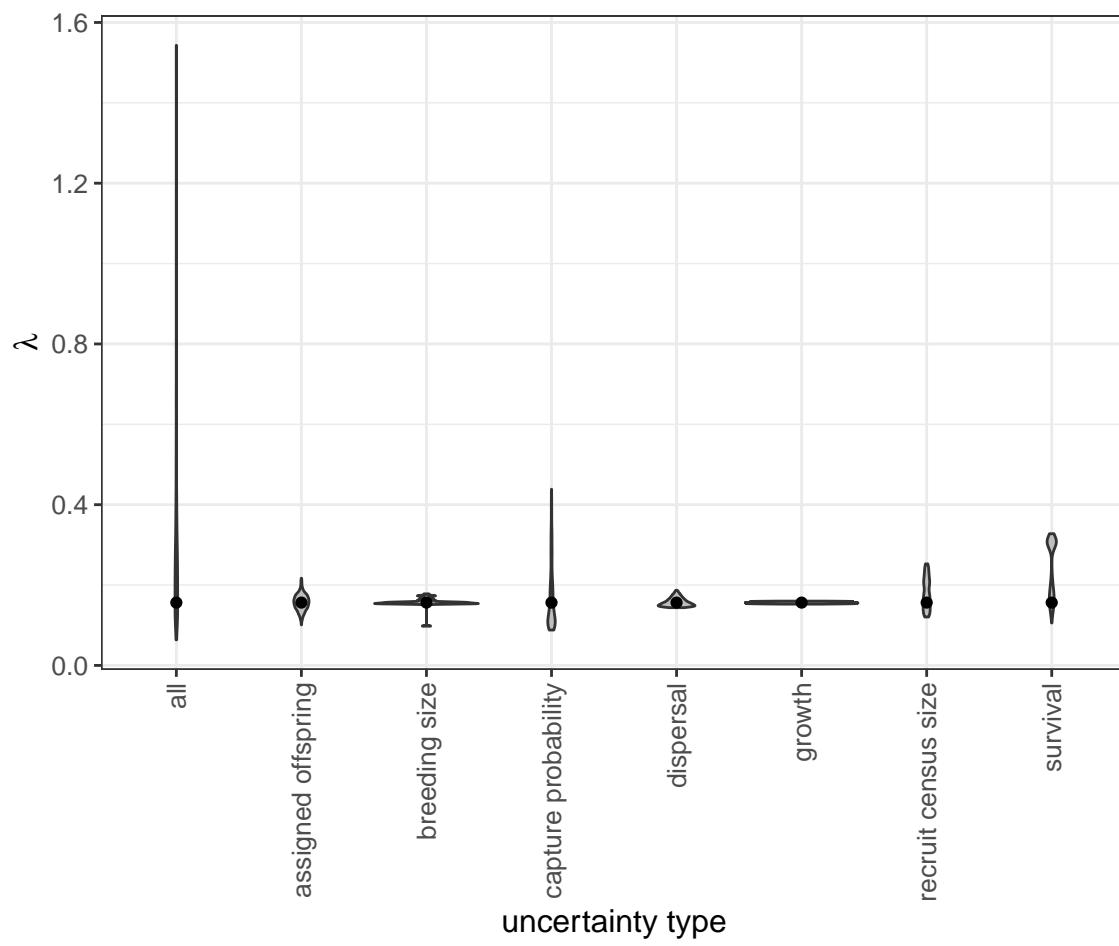


Figure D.13: The contribution of different sources of uncertainty in NP.

## References

- Glenn R Almany, Serge Planes, Simon R Thorrold, Michael L Berumen, Michael Bode, Pablo Saenz-Agudelo, Mary C Bonin, Ashley J Frisch, Hugo B Harrison, Vanessa Messmer, et al. Larval fish dispersal in a coral-reef seascape. *Nature Ecology & Evolution*, 1:0148, 2017.
- Michael Arvedlund, Mark I McCormick, Daphne G Fautin, and Mogens Bildsøe. Host recognition and possible imprinting in the anemonefish *amphiprion melanopus* (pisces: Pomacentridae). *Marine Ecology Progress Series*, 188:207–218, 1999.
- Diana S Baetscher, Eric C Anderson, Elizabeth A Gilbert-Horvath, Daniel P Malone, Emily T Saarman, Mark H Carr, and John Carlos Garza. Dispersal of a nearshore marine fish connects marine reserves and adjacent fished areas along an open coast. *Molecular ecology*, 28(7):1611–1623, 2019.
- Douglas Bates, Martin Mächler, Ben Bolker, and Steve Walker. Fitting linear mixed-effects models using lme4. *Journal of Statistical Software*, 67(1):1–48, 2015. doi: 10.18637/jss.v067.i01.
- David R Bellwood and Rebecca Fisher. Relative swimming speeds in reef fish larvae. *Marine Ecology Progress Series*, 211:299–303, 2001.
- Michael Bode, David H Williamson, Hugo B Harrison, Nick Outram, and Geoffrey P Jones. Estimating dispersal kernels using genetic parentage data. *Methods in Ecology and Evolution*, 9(3):490–501, 2018.

Michael Bode, Jeffrey M. Leis, Luciano B. Mason, David H. Williamson, Hugo B. Harrison, Severine Choukroun, and Geoffrey P. Jones. Successful validation of a larval dispersal model using genetic parentage data. *PLOS Biology*, 17(7):1–13, 07 2019. doi: 10.1371/journal.pbio.3000380. URL <https://doi.org/10.1371/journal.pbio.3000380>.

Louis W Botsford, Alan Hastings, and Steven D Gaines. Dependence of sustainability on the configuration of marine reserves and larval dispersal distance. *Ecology Letters*, 4(2):144–150, 2001a.

Louis W. Botsford, Alan Hastings, and Steven D. Gaines. Dependence of sustainability on the configuration of marine reserves and larval dispersal distance. *Ecology Letters*, 4:144–150, 2001b.

Louis W Botsford, J Wilson White, and Alan Hastings. *Population Dynamics for Conservation*. Oxford University Press, 2019.

Scott C Burgess, Kerry J Nickols, Chris D Griesemer, Lewis AK Barnett, Allison G Dedrick, Erin V Satterthwaite, Lauren Yamane, Steven G Morgan, J Wilson White, and Louis W Botsford. Beyond connectivity: how empirical methods can quantify population persistence to improve marine protected-area design. *Ecological Applications*, 24(2):257–270, 2014.

Peter Buston. Forcible eviction and prevention of recruitment in the clown anemonefish. *Behavioral Ecology*, 14(4):576–582, 2003a.

Peter Buston. Social hierarchies: size and growth modification in clownfish. *Nature*, 424(6945):145–146, 2003b.

Peter M Buston and Cassidy C DAloia. Marine ecology: reaping the benefits of local dispersal. *Current Biology*, 23(9):R351–R353, 2013.

Peter M Buston and Jane Elith. Determinants of reproductive success in dominant pairs of clownfish: a boosted regression tree analysis. *Journal of Animal Ecology*, 80(3):528–538, 2011.

Peter M Buston, Geoffrey P Jones, Serge Planes, and Simon R Thorrold. Probability of successful larval dispersal declines fivefold over 1 km in a coral reef fish. *Proceedings of the Royal Society of London B: Biological Sciences*, page rspb20112041, 2011.

Henry S Carson, Geoffrey S Cook, Paola C López-Duarte, and Lisa A Levin. Evaluating the importance of demographic connectivity in a marine metapopulation. *Ecology*, 92(10):1972–1984, 2011.

Katrina A Catalano, Allison G Dedrick, Michelle Stuart, Jonathan Purtiz, Humberto Montes, Jr., and Malin Pinsky. Interannual variability of genetic connectivity in a coral reef fish *Amphiprion clarkii*. in prep.

MA Coleman, P Cetina-Heredia, M Roughan, M Feng, E van Sebille, and BP Kehler. Anticipating changes to future connectivity within a network of marine protected areas. *Global Change Biology*, 2017.

C. C. D'Aloia, S. M. Bogdanowicz, J. E. Majoris, R. G. Harrison, and P. M. Buston. Self-recruitment in a Caribbean reef fish: a method for approximating dispersal kernels accounting for seascape. *Molecular Ecology*, 22(9):2563–2572, May 2013. ISSN 09621083. doi: 10.1111/mec.12274. URL <http://doi.wiley.com/10.1111/mec.12274>.

Cassidy C D'Aloia, Steven M Bogdanowicz, Robin K Francis, John E Majoris, Richard G Harrison, and Peter M Buston. Patterns, causes, and consequences of marine larval dispersal. *Proceedings of the National Academy of Sciences*, 112(45):13940–13945, 2015.

JK Elliott, JM Elliott, and RN Mariscal. Host selection, location, and association behaviors of anemonefishes in field settlement experiments. *Marine Biology*, 122(3):377–389, 1995.

Stephen P Ellner, Dylan Z Childs, Mark Rees, et al. Data-driven modelling of structured populations. *A practical guide to the Integral Projection Model*. Cham: Springer, 2016.

Lenore Fahrig. How much habitat is enough? *Biological conservation*, 100(1):65–74, 2001.

Daphne Gail Fautin, Gerald R Allen, Gerald Robert Allen, Australia Naturalist, Gerald Robert Allen, and Australie Naturaliste. Field guide to anemonefishes and their host sea anemones. 1992.

Rebecca Fisher. Swimming speeds of larval coral reef fishes: impacts on self-recruitment and dispersal. *Marine Ecology Progress Series*, 285:223–232, 2005.

Emma Fuller, Eleanor Brush, and Malin L Pinsky. The persistence of populations facing climate shifts and harvest. *Ecosphere*, 6(9):1–16, 2015.

Lysel Garavelli, J Wilson White, Iliana Chollett, and Laurent Marcel Chérubin. Population models reveal unexpected patterns of local persistence despite widespread larval dispersal in a highly exploited species. *Conservation Letters*, 11(5):e12567, 2018.

Sarah O Hameed, J Wilson White, Seth H Miller, Kerry J Nickols, and Steven G Morgan. Inverse approach to estimating larval dispersal reveals limited population connectivity along 700 km of wave-swept open coast. *Proceedings of the Royal Society B: Biological Sciences*, 283(1833):20160370, 2016.

Ilkka Hanski. Metapopulation dynamics. *Nature*, 396(6706):41–49, 1998.

Kyle E Harms, S Joseph Wright, Osvaldo Calderón, Andres Hernandez, and Edward Allen Herre. Pervasive density-dependent recruitment enhances seedling diversity in a tropical forest. *Nature*, 404(6777):493–495, 2000.

Hugo B Harrison, David H Williamson, Richard D Evans, Glenn R Almany, Simon R Thorrold, Garry R Russ, Kevin A Feldheim, Lynne Van Herwerden, Serge Planes, Maya Srinivasan, et al. Larval export from marine reserves and the recruitment benefit for fish and fisheries. *Current biology*, 22(11):1023–1028, 2012.

Deborah R Hart and Antonie S Chute. Estimating von bertalanffy growth parameters from growth increment data using a linear mixed-effects model, with an application to the sea scallop *placopecten magellanicus*. *ICES Journal of Marine Science*, 66(10):2165–2175, 2009.

Alan Hastings and Louis W. Botsford. Persistence of spatial populations depends on returning home. *Proceedings of the National Academy of Sciences*, 103:6067–6072, 2006.

Akihisa Hattori and Yasunobu Yanagisawa. Life-history pathways in relation to gonadal sex differentiation in the anemonefish, *amphiprion clarkii*, in temperate waters of japan. *Environmental Biology of Fishes*, 31(2):139–155, 1991.

Kina Hayashi, Katsunori Tachihara, and James Davis Reimer. Low density populations of anemonefish with low replenishment rates on a reef edge with anthropogenic impacts. *Environmental Biology of Fishes*, 102(1):41–54, 2019.

Jordan N. Holtswarth, Shem B. San Jose, Humberto R. Montes Jr., James W. Morley, and Malin. L Pinsky. The reproductive seasonality and fecundity of yellowtail clownfish (*amphiprion clarkii*) off the philippines. *Bulletin of Marine Science*, 93, 2017.

Darren W Johnson, Mark R Christie, Timothy J Pusack, Christopher D Stallings, and Mark A Hixon. Integrating larval connectivity with local demography reveals regional dynamics of a marine metapopulation. *Ecology*, 99(6):1419–1429, 2018.

David M. Kaplan, Louis W. Botsford, Michael R. O'Farrell, Steven D. Gaines, and Salvador Jorgensen. Model-based assessment of persistence in proposed marine protected area designs. *Ecological Applications*, 19(2):433–448, March 2009. ISSN 1051-0761. doi: 10.1890/07-1705.1. URL <http://www.esajournals.org/doi/abs/10.1890/07-1705.1>.

J.L. Laake. RMark: An r interface for analysis of capture-recapture data with MARK. AFSC Processed Rep. 2013-01, Alaska Fish. Sci. Cent., NOAA, Natl. Mar. Fish. Serv., Seattle, WA, 2013. URL <http://www.afsc.noaa.gov/Publications/ProcRpt/PR2013-01.pdf>.

David Lecchini, Serge Planes, and René Galzin. Experimental assessment of sensory modalities of coral-reef fish larvae in the recognition of their settlement habitat. *Behavioral Ecology and Sociobiology*, 58(1):18–26, 2005.

Dale R Lockwood, Alan Hastings, and Louis W Botsford. The effects of dispersal patterns on marine reserves: does the tail wag the dog? *Theoretical population biology*, 61(3):297–309, 2002.

Piotr Nowicki and Vladimir Vrabec. Evidence for positive density-dependent emigration in butterfly metapopulations. *Oecologia*, 167(3):657, 2011.

Piotr Nowicki, Simona Bonelli, Francesca Barbero, and Emilio Balletto. Relative importance of density-dependent regulation and environmental stochasticity for butterfly population dynamics. *Oecologia*, 161(2):227–239, 2009.

Haruki Ochi. Mating behavior and sex change of the anemonefish, *amphiprion clarkii*, in the temperate waters of southern japan. *Environmental Biology of Fishes*, 26(4):257–275, 1989.

Malin L Pinsky, Humberto R Montes Jr, and Stephen R Palumbi. Using isolation by distance and effective density to estimate dispersal scales in anemonefish. *Evolution*, 64(9):2688–2700, 2010.

BJ Puckett and DB Eggleston. Metapopulation dynamics guide marine reserve design: importance of connectivity, demographics, and stock enhancement. *Ecosphere*, 7(6), 2016.

Nicholas L Rodenhouse, T Scott Sillett, Patrick J Doran, and Richard T Holmes. Multiple density-dependence mechanisms regulate a migratory bird population during the breeding season. *Proceedings of the Royal Society of London. Series B: Biological Sciences*, 270(1529):2105–2110, 2003.

Océane C Salles, Glenn R Almany, Michael L Berumen, Geoffrey P Jones, Pablo Saenz-Agudelo, Maya Srinivasan, Simon R Thorrold, Benoit Pujol, and Serge Planes. Strong habitat and weak genetic effects shape the lifetime reproductive success in a wild clownfish population. *Ecology letters*, 23(2):265–273, 2020.

Océane C. Salles, Jeffrey A. Maynard, Marc Joannides, Corentin M. Barbu, Pablo Saenz-Agudelo, Glenn R. Almany, Michael L. Berumen, Simon R. Thorrold, Geoffrey P. Jones, and Serge Planes. Coral reef fish populations can persist without immigration. *Proceedings of the Royal Society B: Biological Sciences*, 282(1819):

20151311, November 2015. ISSN 0962-8452, 1471-2954. doi: 10.1098/rspb.2015.1311. URL <http://rspb.royalsocietypublishing.org/lookup/doi/10.1098/rspb.2015.1311>.

James NM Smith and Jessica J Hellmann. Population persistence in fragmented landscapes. *Trends in Ecology & Evolution*, 17(9):397–399, 2002.

Diane M Thompson, J Kleypas, F Castruccio, Enrique N Curchitser, Malin L Pinsky, B Jönsson, and James R Watson. Variability in oceanographic barriers to coral larval dispersal: Do currents shape biodiversity? *Progress in oceanography*, 165: 110–122, 2018.

Nick Tolimieri and Phillip S Levin. The roles of fishing and climate in the population dynamics of bocaccio rockfish. *Ecological Applications*, 15(2):458–468, 2005.

Mark JA Vermeij and Stuart A Sandin. Density-dependent settlement and mortality structure the earliest life phases of a coral population. *Ecology*, 89(7):1994–2004, 2008.

Robert R Warner and Peter L Chesson. Coexistence mediated by recruitment fluctuations: a field guide to the storage effect. *The American Naturalist*, 125(6): 769–787, 1985.

J. Wilson White, Mark H Carr, Jennifer E Caselle, Libe Washburn, C. Brock Woodson, Stephen R Palumbi, Peter M Carlson, Robert R Warner, Bruce A Menge, John A Barth, Carol A Blanchette, Peter T Raimondi, and Kristen Milligan. Con-

nectivity, dispersal, and recruitment: Connecting benthic communities and the coastal ocean. *Oceanography*, 32(3):50–59, 2019.

Jw White, Lw Botsford, A Hastings, and Jl Largier. Population persistence in marine reserve networks: incorporating spatial heterogeneities in larval dispersal. *Marine Ecology Progress Series*, 398:49–67, January 2010. ISSN 0171-8630, 1616-1599. doi: 10.3354/meps08327. URL <http://www.int-res.com/abstracts/meps/v398/p49-67/>.

Adam Yawdoszyn. Fecundity in clownfish. in prep.